NASA

HIGH TEMPERATURE STATIC STRAIN GAGE ALLOY DEVELOPMENT PROGRAM

By
C.O. Hulse, R.S. Bailey
and F.D. Lemkey

UNITED TECHNOLOGIES RESEARCH CENTER

High Temperature Static Strain Gage
Alloy Development Program

by

C. O. Hulse, R. S. Bailey, and F. D. Lemkey

United Technologies Research Center

prepared for

National Aeronautics and Space Administration

NASA Lewis Research Center
Contract NAS3-23169

ABSTRACT

The literature, applicable theory and finally an experimental program were used to identify new candidate alloy systems for use as the electrical resistance elements in static strain gages up to 1250K. The program goals were 50 hours of use in the environment of a test stand gas turbine engine with measurement accuracies equal to or better than 10 percent of full scale for strains up to $\pm$ 2000 microstrain. As part of this effort, a computerized electrical resistance measurement system was constructed for use at temperatures between 300K and 1250K and heating and cooling rates of 250K/min and 10K/min. The two best alloys were Fe-10.6Cr-11.9Al and Pd-13Cr in weight percent. Although significant progress was made, it was concluded that a considerable additional effort would be needed to fully optimize and evaluate these candidate systems.

High Temperature Static Strain Gage
Alloy Development Program

TABLE OF CONTENTS

1.0 SUMMARY

A one-year development program was conducted to identify two resistive strain gage alloy candidates for use in gas turbine test stand engines at temperatures up to 1250K. These alloys were to be usable as static strain gages in the environment of a gas turbine engine with lifetimes of at least 50 hours at maximum strain levels of ± 2,000 με with errors of no more than plus or minus 10 percent of full scale. The final strain gages were to measure no more than 3 mm on a side for use on smaller airfoils, with total gage thicknesses not to exceed 0.5 mm for a wire gage or 0.2 mm for a foil type strain gage.

After an initial literature survey and analysis, ten alloy candidates were identified using as a ranking system the product of relative numerical values estimated for key material properties. After some preliminary testing, a review and discussion with NASA, these ten were reduced to six candidates for further evaluation and development. The original fabrication plan to prepare the alloys by sputtering was replaced for reasons of speed and economy by drop-casting the arc-melted alloys to form rods inside ceramic tubes. For making resistance measurements, these rods were subsequently ground and polished to form strips, typically 0.056 x 0.444 x 12.7 cm long. A resistance measurement facility was constructed which was capable of making precision measurements up to 1250K at constant temperatures or at rates of heating and cooling from 10 to 250K/min in an argon atmosphere. The system used the four-wire resistance measurement approach with a high quality voltmeter, scanner, and a computer to measure and process the data.

A selection process was developed and used to compare the six final candidate systems: Pt-Pd-Mo, Pd-Ag-Mo, Ni-Si-Cr, Pd-Cr, Pt-W and Fe-Cr-Al. The Mo-Ag-Pd system was dropped from the list of six final candidate systems when problems with liquid immiscibility were encountered. The Nicrosil, Ni-Si-Cr, system was also dropped because its resistance did not vary linearly with temperature and it had a relatively high thermal coefficient of resistivity. A series of 32 different alloy samples of the other candidate systems were prepared and evaluated in an iterative process which involved measurements of electrical drift at 1250K and measurements of the thermal coefficient of resistivity over the range from 300 to 1250K. Measurements were made of the sensitivity of the electrical resistance to rates of heating and cooling from 10 to 250K/min and the repeatabilities of resistance over the range 300 to 1250K. The compositions, the stress-strain behavior, melting points, the coefficients of thermal expansion, creep and the resistances to oxidation of the best alloy of each type were also measured.

The two best alloy candidates finally identified were Pd-13Cr and Fe-10.6Cr-11.9Al in weight percent. It was concluded that the optional second year of this program to fabricate and test complete strain gage systems using the alloys developed during the first year should be delayed until after an additional effort had been made to further optimize the two best alloy systems identified.

2.0 INTRODUCTION

The purpose of this effort was to advance our abilities to design and produce improved gas turbine engines through the development of an improved static strain gage. This improved strain gage was to be able to determine the elastic strains in gas turbine parts within an engine running on a test stand by measurements of the relative changes in the electrical resistance of a resistor network attached to the component of interest. In order to operate properly, this sensor system, including the leadwires, would have to be electrically insulated from the turbine part, be electrically stable and also able to survive the chemical and thermal environments and the high centrifugal forces present within these engines.

The major technical goal of this strain gage development program was a useful lifetime of at least 50 hours at temperatures up to 1250K. The temperatures of use would range from 1000K to 1250K with maximum strain levels of ±2000 microstrains at 1250K and ±3000 microstrains at 1000K. An accuracy goal of ±10 percent of full scale was also established. The sensor size requirements were 3mm square for smaller airfoils while 6 mm square would be acceptable for larger airfoils. The maximum thickness was not to exceed 0.5 mm for a wire system and 0.2 mm for a thin film system.

This work was part of a much larger effort by the National Aeronautics and Space Administration called the HOST program. The goal of the HOST program is to improve the technology in the hot sections of gas turbine engines. The HOST program is to continue on into the 1990's, supporting a variety of studies by various aerospace contractors and by others at NASA Research Centers. This contract, NAS3-23169, is one of a number of early programs in the HOST effort directed toward the development of improved sensors for use inside gas turbine engines. The goal of the first year of this effort was to identify several new and improved alloys for use as the strain sensing elements. An optional second year of effort was to demonstrate the use of two of these alloys in a complete strain gage system which would satisfy the goals mentioned above.

Strain gage systems which employ platinum alloy wires embedded in flame-sprayed alumina have been used successfully in gas turbine engines to measure dynamic strains up to temperatures as high as 1250K. Dynamic strains, however, are much easier to measure because only relative values are required over very short time spans. Apparent strain corrections due to the various effects of temperature on the voltages measured and drifts in resistance with time relative to a reference value of zero strain do not have to be considered.

The static strain measurement problem for this application is especially difficult because of the high temperatures involved compared to the reference condition of room temperature at zero strain. This requirement for stability with both time and temperature change is further compounded by the fact that temperatures on the surfaces of gas turbine hardware are difficult to determine, uncertainties of ±10K being common. The presence of high thermal gradients further compounds this problem. These uncertainties make apparent strain corrections from prior calibration runs especially difficult and generates a requirement that the thermal coefficient of resistivity, (TCR), be extremely low, of the order of 20 ppm/K

$$TCR = \frac{\Delta R/R}{\Delta T} \leq 20 \times 10^{-6}/K \qquad (1)$$

where

    ΔR = Change in Electrical Resistance
    R   = Electrical Resistance
    T   = Temperature.

There has been an increasing recognition that if significant progress is to be made in the development of improved strain gages, completely new alloys must be identified for use as the sensing elements. The Ni-20 Cr alloy (composition in weight percent) is the most widely used sensor composition presently used in gas turbine engines. It's maximum use temperature is approximately 800K which is far below the temperature requirements of this program. The resistance of this alloy is non-linear with temperature and when heated above 800K the resistance becomes sensitive to the rates of heating and cooling.

Fine wires of a commercial heating wire composition, Fe-22.0Cr-5.7Al-0.5Co[*] have also been used to measure strains at temperatures up to about 1000K. The resistance of this wire is also nonlinear with temperature and sensitive to the rates of heating and cooling. A demonstration of the usefulness of this alloy as compared with strains measured using a laser speckle technique is the subject of a current NASA contract NAS3-23690 (Reference 1). The earlier work of Lemcoe and coworkers with other FeCrAl type alloys under NASA funding is also important in showing that other alloys in this system may be used as strain gage elements (References 2 and 3). More recent work under NASA contract NAS3-22126 showed that above about 1000K, the Fe-22.0Cr-5.7Al-0.5Co alloy underwent metallurgical changes which made it unsuitable for use as a strain gage sensor (Reference 4).

---

[*]Kanthal A-1, Kanthal Corp., Bethel, Connecticut

Because of the need for chemical stability, especially the need to resist oxidation at high temperatures, investigations have also been made of the potential usefulness of precious metal alloys as strain gage sensors. The work of Bertodo is by far the most outstanding (References 5 to 9) although the important work of Esterling should also be mentioned (Reference 10). A more complete discussion of prior work and the metallurgical problems involved are reviewed in Section 3.1 of this report.

This program has generated data on the electrical and mechanical properties of a variety of relatively stable materials. A technique was developed to easily prepare test samples of a variety of compositions and an experimental facility was developed to measure their electrical resistivities up to 1250K under both dynamic and static thermal conditions. Some improved materials were identified which may be useful not only as strain gage sensors but also in other electrical circuits where electrical stability over a significant range of elevated temperatures is important.

3.0 INITIAL EFFORTS AND PLANS

The initial task in this program was to conduct a study to identify alloys which might be suitable for use as the resistance sensing element in static strain gages capable of operating to 1250K in the environment inside a gas turbine engine. This effort included: (1) a literature search to identify existing materials candidates, (2) a materials analysis to determine new alloys and (3) consultation with recognized materials experts. A minimum of ten alloys were to be identified and recommended to the NASA Project Manager using a merit ranking system which was to be developed as a part of the program. After a review and discussion of the ten alloys, the NASA Project Manager was to select six candidates for experimental evaluation and development in this program.

3.1 Literature Review

The Research Center library literature search computer was used to provide a listing of literature titles associated with strain gages, key materials properties and high temperature alloy families. These listings were reviewed and appropriate titles were ordered by the library. Over 140 articles were read and discussed. Professor Hans Nowotny, an internationally known materials scientist presently associated with the University of Connecticut and a consultant on this contract, was also involved in this effort. A bibliography of these sources, included in this report as Appendix I, was also prepared and sent to the NASA Project Manager.

Since the first attempt to measure strain by bonding a resistor network to a surface in 1938, many people have published descriptions of their investigations. The ASTM Symposium on this subject in 1957 (Reference 11) describes some of the best work up to that date. Most of the work to develop gages for elevated temperature use has centered on the use of alloys of the transition metals: Ni-Cr, Ni-Cr-Al, Fe-Cr-Al and Ni-Cr-Fe-Al (Ref. 5, 10, 12). These alloys have relatively good resistances to oxidation and generally exhibit nonlinear resistance versus temperature behavior with relatively low temperature coefficients of resistance (TCR). These alloys have a tendency to undergo solid state transformations, apparently ordering reactions. The transition metals are unusual in that ordering reactions tend to increase the resistance of the alloy instead of decreasing the resistance which is the normal result of ordering reactions (Reference 10).

A number of concepts have been advanced to overcome or reduce the effects of high TCR's by methods which avoid the development of a special new alloy. Attempts have been made to fabricate a coated wire system as a way to combine materials with positive and negative TCR's (Reference 2, 3, and 13) and to combine alloys in series which have either opposite or widely differing TCR's

(Reference 5 and 14). A summary of various possible temperature-compensation circuits is contained in Reference 7.

In recent Chinese work by Wu, et al (Reference 15) a new Fe-Cr-Al-V-Ti-Y strain gage alloy was developed with improved properties. These alloys have been given special drawing and thermal pretreatments to optimize their properties. The behavior of these strain gages is presently being evaluated in the United States.

Considerable attention has been placed on alloys of the precious metals because of their high melting points and generally good resistances to oxidation. The best alloys which resulted from the extensive alloy development work by Bertodo (References 5 through 9) are Pt-8.5W and 45 Pt-45 Pd and 10 Mo in weight percent. Additional work by other investigators as well as Bertodo, summarized in Reference 9, has suggested that metallurgical transformations (ordering reactions) can also occur in the Pt-(8-10)W alloys at low temperatures. Although Bertodo indicates that alloys of these types should be usable up to 1000°C (1273K), there are concerns about the oxidation resistance of alloys of these types which contain components which form volatile metal oxides. For example, Weise and Foster, in their work to evaluate strain gages for use in high temperature fatigue (Reference 13), conclude that because of oxidation, Pt-8W should not be used above 750K.

3.2 Sample Fabrication Plan

Because it was expected that the sputtering technique would be selected as the fabrication approach to be used in making complete strain gage systems, it was planned also to use this technique to prepare samples of the different alloy candidates. Relatively coarse resistor networks with sizeable end tabs were to be sputtered on commercially available thin alumina substrates, typically cut into plates 7.5 X 2.5 X 0.025 cm. In order to evaluate the thermal sensitivity of the electrical resistance of the alloy sample independent of the thermal expansion of the alumina substrate, the resistive network was to be sputtered on an area of the substrate which had been precoated with an evaporated film of carbon or some other organic coating. A subsequent heating in air should burn off the carbon to leave a "free" sputtered network whose measured electrical resistance should only reflect its intrinsic sensitivity to temperature.

Non-precious metal sputtering targets were to be cast to shape using the melting and casting facilities available at the Research Center. Precious metal alloy targets were to be prepared by using a composite target approach being developed at the Commercial Products Division of Pratt and Whitney. In this approach, a disk of a non-precious metal, such as tungsten, is used as a substrate on to which are sputtered areas of precious metals from pure precious

metal targets. The composition of the alloy sputtered from this target can be varied by having used masks with different hole sizes and by using different pure precious metal sputtering targets. In the final sputtering step using this composite target, the various elements in the alloy are mixed as they travel simultaneously from different areas of the target to the same spot in the sample.

After the program started, it was discovered that unattached sputtered coatings were difficult to prepare. It was also realized that it was going to be difficult to accomplish all the sputtering runs under optimum conditions that we would like to have done in this program within the necessary time. A drop casting technique for sample fabrication, described more fully in Section 4.1, was then developed. This approach permitted test samples to be fabricated much more quickly and with less expense. This also permitted many more alloy iteration to be accomplished than was required by the Statement of Work for this program.

3.3 Test Plan

One of the requirements of the Statement of Work was that a test plan should be developed to describe the experiments which would be used to evaluate the various alloys that were prepared. The first part of the test plan described a limited series of critical property evaluations that would be used to screen the six alloy types selected by the NASA Program Manager down to four alloys. At least one iteration of composition was required of each alloy type to see if better properties could be developed. The properties evaluated were: (a) the repeatability of resistivity (b) the thermal coefficient of resistivity over the range of temperature from 300 to 1250K, (c) the effect of rate of change of temperature (10, 50 and 250K/min) on the repeatability and the thermal coefficient of resistivity and (d) the drift or change in resistivity during a 3 hour soak at 1250K.

In order to assure that the properties measured were not showing the effects of grain growth or similar processes, test samples were to be given a pretest stabilization heat in argon at 1473K, well above the top test temperature of 1250K. Arc-melted samples of potential alloy compositions were also to be mounted, polished and examined metallographically and/or with the Scanning Electron Microscope (SEM) after being slowly cooled after these heat soaks to determine if any second phase precipitates were present. Compositions containing precipitates which might undergo exsolution or resolution processes during different thermal exposures were not considered to be of interest.

The second part of the test plan was to measure some additional properties of the four final alloys selected which would be important in their use as strain gages, but perhaps not as critical as the properties measured earlier. These properties were: (a) chemical composition, (b) melting point, (c) stress-strain curves, (d) the coefficient of thermal expansion, (e) creep strength and (f) resistance to oxidation.

The final part of the test plan was to prepare one alloy as a strain gage film by the sputtering process and to measure some of its properties in that form. The properties to be measured were resistivity, the thermal coefficient of resistivity and the drift of electrical resistance at 1250K. The purpose of this work was to verify that the properties of the alloys prepared by casting from the melt could be correlated directly with the properties of materials prepared using the sputtering process.

4.0 EXPERIMENTAL

4.1 Sample Preparation

As mentioned in Section 3.2, the initial work plan was to prepare the various alloy samples by sputtering on thin (0.025 cm) alumina plates commercially available for use as electronic substrates. The sputtering approach was subsequently discarded in favor of a drop casting approach which was developed to prepare different alloy samples much more quickly and inexpensively. The sputtering approach unfortunately required the fabrication of a new alloy target for each different alloy prepared and also the use of very specialized equipment for each time consuming sputtering run.

In order to prepare samples by drop casting, a commercial* three electrode arc melter was first used to prepare homogenized molten buttons of premeasured compositions. The initial elemental components all had purities of at least 99.9 weight percent. These buttons were typically turned over and remelted three times before the casting step to ensure uniform mixing. The flat copper water-cooled anvil in the arc melter was then replaced by another anvil with a vertical, centered hole. The hole contained a ceramic tube into which the molten alloy would cast. The alloy button, with the bottom surface polished flat, was placed over the hole and melted again. When the bottom of the button which was against the water-cooled hearth was melted, the small argon over pressure in the melting chamber became sufficient to blow the melt into the tube where it immediately solidified as a rod.

The FeCrAl and Pd alloy samples were cast inside fused silica tubes while all the other alloys were cast inside alumina tubes in order to avoid chemical reactions. Because of the smoothness of the inside surfaces of the fused silica tubes and the low coefficient of thermal expansion, the test samples normally slid freely out of the silica tubes. When alumina tubes were used, the ceramic usually had to be broken in order to remove the samples. Typical cast samples were from 8 to 18 cm long and 0.452 cm in diameter.

In order to develop higher voltages in samples prepared for resistance measurements, these cast rods were subsequently reduced by grinding and polishing to strips which were 0.056 cm thick. A special hardened steel plate containing flat bottomed slots of different depths was prepared in order to accomplish this task. Rods were cemented into one of these slots with a thermal wax (bee's wax plus rosin) and then the plate was manually held on a grinding or a polishing wheel until all of the material which protruded above the slot was removed in a uniform fashion. In order to avoid the presence of any of the small shrinkage voids which were sometimes present at the centers of the rods, the sample strip was normally taken slightly off center from the original cast rod.

---

*Centorr Associates, Suncook, N.H.

Samples for tensile and creep testing were prepared by waxing the cast cylindrical rods on a flat plate and grinding away a reduced section in the center third of the sample rod. In order to prepare a more symmetrical sample, the rod had to be turned over, recemented, and ground again in order to form an approximately centered gage section, typically 0.056 cm thick and as wide as the original diameter of the cast rod.

Before testing, the samples were normally heated for several hours in tank argon at a temperature well above one-half of their absolute melting temperatures. The oxygen concentration present in argon from this source was typically 1 to 2 ppm. This was done in an attempt to homogenize their chemical compositions and to produce an annealed sample with a stable grain structure. For these treatments, the samples were held inside small alumina tubes which were wrapped in Mo or Ta foils in order to getter away any oxygen or water vapor which might have been present.

4.2   Resistance Measurements

Measurement of electrical resistance at various constant or changing temperatures were made using a testing facility initially developed for measuring the electrical resistances of 0.0025 cm diameter FeCrAl alloy* wires on prior NASA Contract NAS3-22126. The furnace used in this facillity consisted of a 2.5 cm outer diameter tube of either stainless steel or Hastalloy-X, which was 21.6 cm long and split in half lengthwise for ease of sample set up. The system also included a power supply and control system capable of supplying up to 1500 amps of AC current to the tube heater through 2.5 cm wide water-cooled copper electrodes clamped to each end of this heater tube. The electrode which supplied furnace power to one end of the heater tube was mounted on ball bearings in order to accommodate the thermal expansions of the tube during heating and cooling. A diagramatic view of the test system showing the position of the test sample relative to the heater tube is presented in Figure 1.

The complete tube furnace system was enclosed in a sealed plastic box which was normally purged continuously with building argon in order to prevent oxidation of the sample. Although not measured, the oxygen concentration in the building argon, which is piped into the laboratory from a general source, is believed to be higher than that present in the argon from an individual tank.

Good electrical contact with the samples was obtained by physically clamping a folded over 0.25 mm thick sheet of platinum against the sample. The clamps which supplied these forces consisted of double sets of B-1900 nickel base super-

---

*Kanthal A-1, Kanthal Corp.

alloy beams which extended into the tube heater. Each of these two clamps supplied a calculated clamping force of at least 220 N at 5 cm inside the tube over the full range of test temperatures from 298 to 1250K. These forces were developed by tightening a bolt just outside the end of the heater tube between the two cantilevered clamping beams.

In the initial plan, both of the sputtered electrode tabs were to be at the same end of the tube furnace so that the two sets of clamping beams were beside each other at the same end of the furnace. When the sample was changed to a thin strip, the position of the clamps was changed so that they were at opposite ends of the furnace. When this change was made, one of the pairs of clamping electrodes was suspended from a spring system in an attempt to avoid placing any loads on the sample strip which might generate undefined resistance change effects during the tests.

The temperature of the furnace was measured using a 0.005 cm diameter Type K wire thermocouple located just below the sample at the center of the furnace. This thermocouple was connected to a controller* which could be programmed** to drive the system through a series of heating and cooling cycles at 10, 50 and 250 K/min or to hold the tube furnace at a constant temperature of 1250K in order to measure the stabiity of the electrical resistance of the sample. When cooling at 250K/min, the programmer automatically turned on helium jets below about 600K which helped to cool the heater tube to maintain such a high rate of cooling at low temperatures.

The electrical resistance of the samples were measured using the four wire technique. Two platinum wires 0.005 cm in diameter were spot welded to the sample strip to measure the voltage drop across a 3 cm section of the sample at the center of the tube furnace. In order to accurately measure the current through the sample, which was typically about 1.6 amps, a decade resistance box was placed in series with the sample. Measurement of the voltages across this known resistance provided a measure of the current through the sample. The voltage drop across the reference decade resistance box and the voltage drop across the sample were fed through a scanner* to a two pen strip chart recorder. One pen recorded through the scanner, alternately, the voltage drop across the sample and then that across the reference decade resistance box. The second pen continuously recorded the sample temperature as measured by a 0.005 cm dia Type K thermocouple spot welded to the center of the sample. By use of the zero suppression feature of the recorder and careful selection of the value of the reference resistor, it was possible to make both of these measurement on a 1 mV full scale range for maximum sensitivity. These charts were read manually and the data entered into a HP 9845 computer for subsequent data processing and plotting.

---

* Research Incorporated
** Research Incorporated

As the program progressed it became evident that improvements would have to be made in the resistance measurement system in order to attain the high levels of accuracy and stability required for the work. It was determined, for example, that the decade resistance box was sensitive to the temperatures in the laboratory which could vary appreciably, especially over night or on weekends. The decade box was replaced with a single high precision resistor which was bolted to a water-cooled aluminum plate for thermal stability. A complete computer system was then obtained to enable more accurate measurements to be made. The system consisted of a high precision voltmeter, a high speed scanning system, a programmable integral power supply and a minicomputer to store and process the data*. The data measurement program consisted of an initial measurement of the thermocouple voltage followed by a series of 20 readings alternately of the voltage drops across the sample and that of the reference resistor and, finally, a measurement of the thermocouple voltage. The average of each of these three different types of readings were determined and used to compute the relative change in resistance at that temperature relative to an initial resistance value measured at the start of the run.

4.3   Stress-Strain and Creep Testing

Measurements of stress-strain behavior and creep testing were accomplished using commercial high temperature wedge grips made of MAR-M247**. The cylindrical ends of the samples, prepared as described in Section 4.1 above, were gripped by serrated wedges which could slide to accommodate small changes in sample diameters or to increase the gripping forces as needed. All tests were made in air using a Tinius Olsen Universal Testing machine. Strain gages were used to measure strain during stress versus strain measurements made at room temperatures. Two gages were used on each sample in order to cancel out any possible effects due to bending. In elevated temperature testing, the sample gage lengths were taken as the total length of the reduced section, typically about 5 centimeters, and the strain was computed from measurements of cross head motion. The creep curves were all obtained at 1250K over a period of approximately 3 hours. The creep stresses selected were approximately equal to one-half of the yield stresses determined in separate tests at 1250K. Sample temperatures were measured using a Type K thermocouple which touched the sample at the center of the gage length.

4.4   Thermal Expansion and Melting Points

The thermal expansions of these alloys were measured in air using a fused silica dilatometer. The expansions and contractions of the samples were

---

* Hewlett Packard, 305A Data Acquisition system, 9826A computer and 6002A power supply.
**Applied Test Systems, Saxonberg, P.A.

continuously recorded on an X-Y plotter as a function of temperature from the output of an LVDT transducer located just above the furnace. Typical sample dimensions were 0.45 cm in diameter and 1.9 cm long. The samples were heated and cooled at 2.0 K/min and three consecutive cycles were normally run in order to make sure that the measurement system was fully stabilized, the last run being taken as the most accurate.

The melting points of these alloys were determined in argon by supporting a length of cast rod in two notches in the end of a one-inch diameter alumina tube vertically positioned in the center of an R. F. susceptor. The melting point was determined as the temperature at the end of the alumina tube when the sample melted and fell down the tube.

5.0 RESULTS

5.1 Analysis

Certain material properties can be identified as necessary in order to meet the goals of this program. The primary interest is in alloys which have a high electrical resistivity which is very stable with time at high temperatures. Additional requirements are a low thermal coefficient of resistivity and excellent resistance to oxidation. Apparent strains are errors in computed strains caused by changes in electrical resistance which are not caused by elastic or plastic strains in the substrate. Materials with the above properties will have the minimum errors due to apparent strain effects caused by incorrect temperature measurement, high thermal gradients, oxidation and microstructural instabilities.

Rigorous theoretical solutions to describe the behavior of an electron in a solid, are not available except for the cases of several simple, pure elements. Unfortunately, the resistivities of elemental conductors are far too low and the thermal coefficients of resistance (TCR's) are much to high for them to be considered as candidates in this program. As the temperature of a crystal lattice is increased, the thermal motion of the atoms around their crystal sites increases. This causes these atoms to become more effective in scattering or interfering with the drift of electrons through the lattice. Increases in resistivity due to this effect are directly proportional to the absolute temperature. In order to overcome this sensitivity of resistance to temperture, some additional mechanisms of electron scattering must employed which are either temperature independent or change in the reverse sense with temperature. The most practical approach is to employ temperature independent mechanisms whose contributions are so large that the intrinsic lattice effects mentioned above become unimportant.

In the absence of: (1) a rigorous theory from which the electrical properties of alloys can be derived, and (2) reliable electrical data for many alloy systems, a number of geneal rules concerning the electrical properties of dilute alloys have been developed which were used to guide our efforts. These rules are summarized below:

Matthieson's Rule

Resistivity = $\rho_o + \rho_T$

ρ_T is temperature dependent resistivity due to lattice vibration scattering

ρ_o is temperature independent resistivity due to defects such as alloying elements.

LeChatelier - Guertler's Rule

Temperature Coefficient of resistance, TCR, of an alloy is lower than that of a pure metal. (This follows from Matthiesen's Rule.)

Dellinger's Rule

The product of   and TCR tends to be a constant in an alloy system as composition is changed. Choose an alloying element which increases   strongly in order to decrease the TCR strongly.

Linde's Rule

For dilute alloys, $\Delta^\frown$ is proportional to V_x^2. Choose high V_x to increase $\frown$. V = Valence, x = alloying element.

Norbury's Rule

For dilute alloys in any one row of the Periodic Table, $(N-N_x)^2$ is proportional to ρ; where N is atomic number, choose x for high $N-N_x$ for the maximum increase in ρ.

Oxidation of Alloys

The oxidation rate of an alloy tends to be like that of the principal (host) element provided the alloying element does not form an adherent film which resists the diffusion of oxygen.

One method to increase the scattering of electrons would be to add significant amounts of second phase particles. This approach is undesirable, however, because it would necessarily include exsolution and resolution processes which will change as a function of both temperature and time. The expected result would be significant drifts in resistivity with time and an inability to obtain reproducible properties.

The mean free path of an electron in a crystal lattice is of the same order as the atomic spacing. This means that even very small second phase precipitates would not, in and of themselves, be effective as scattering centers. The primary effect of a second phase would be to act as reservoir from which atoms could be obtained to change the concentrations of elements in solid solution. One immediate criterion in our search, therefore, is that our gage alloy should be single phase over the complete temperature range of interest.

Another approach to increase the resistivity and lower the TCR might be to cold work the alloy to produce grain boundaries, dislocation tangles, point defects, internal stresses and subgrain boundaries. If this approach is taken, great care must be taken to assure that all of these electron scattering defects are stable and that they will not be changing by time dependent processes during use at elevated temperatures. The best way to achieve this would be by a long term annealing at some temperature slightly above the maximum use temperature. In this event, the concentration of these defects would probably be reduced and those that remained would probably not be able to contribute a very large beneficial effect.

An alternative approach might be to produce our alloys by some technique which forces the presence of a highly disordered state. The so called Mooij alloys would be an example of this idea (Reference 16). These "glassy" type materials can have very high resistivities and very low, even negative, TCR's. Mooij has suggested that negative TCR's may be caused by the presence of "activated complexes" which can generate additional conduction electrons at elevated tempertures. Although this approach is not useful because these alloys become unstable at elevated temperatures, they do illustrate Dellinger's Rule and that very low TCR's are a direct result of highly disordered structures.

Another approach to reduce the TCR would be to examine the properties of ceramic materials or materials which contain a mixture of metallic and ionic or covalent bonding, such as Cerium Sulfide. Ionic and covalently bonded materials tend to become better electrical conductors as the temperature is raised and more electrons are activated up into the conduction bands. Although some of these materials were reviewed, it was decided that this was too long term a project and that it was not likely to produce viable candidates within the necessary time frame of this program.

In our opinion, the best and most direct approach to increase the resistance and reduce the TCR is by preparing solid solutions whose solute concentrations cannot change with temperature. This leads to questions of which alloying elements to select. Neglecting environmental stability factors, the following guidelines may be used:

1. The differences in atomic radii for appreciable solubilities should not exceed 10 percent.

2. Electronegativities should be as close as possible for maximum solubility, differences greater than one half unit tend to favor compound formation.

3. Multiple valent solute elements should be preferred.

4. The elements should be separated by as much as possible in the Periodic Table, especially along the row.

5. Transition elements are particularly desirable as solute additions because they have vacant inner electron shells which make them more effective as scattering centers.

A basic difficulty that is encountered in the development of lattice disorder by extensive solid solution is that, as the temperature is decreased, ordering transformations may occur in order to lower the free energy of the system. Figure 2 shows a classic example of ordering in the copper-gold system and how significant these effects can be. Note that in this case, only small changes in compositions can result in the presence or complete absence of this effect. The basic experimental objective in finding alloys with high resistances and low TCR's, therefore, reduces to the discovery of single phase solid solution alloys which contain the highest possible concentrations of the most different elements in the largest variety possible which will not undergo order-disorder type reactions within the temperature and time limits defined by the program goals.

5.2 Alloy Selection and Evaluation

In order to evaluate the potential usefulness of various alloy candidates, a numerical system of comparison was developed. A number of key factors or properties for this application were identified, and high or low numbers assigned depending on the desirability of that property. Because it was felt that certain alloy factors were of more importance than others, the numerical importance of the more significant properties were extended in range so that greater weighting factors could be attained. Table I lists the properties used in this evaluation together with the range of relative values which could be assigned. A larger numerical value corresponded to a more desirable value for the property.

Most of the factors in Table I are of obvious importance. The Judgement Factor was as a more general term which included such factors as risks, ductility or brittleness and experience with the alloy.

When the upper value of these factors are added their sum is 100. It was found, however, that the numerical separation between the sums of the candidates' properties tended to be relatively small. Each candidate tended to score well in some property which would then off-set a relatively poor score in some other property. In order to provide a clearer separation and to better account for the fact that the importance of all the factors are interconnected, the following product ranking formula was used with the symbols representing the properties listed in Table I.

$$\text{Rank} = (R_p) \cdot (O) \cdot (\rho) \cdot (TCR) \cdot (\Delta\varepsilon) \cdot (\Delta\alpha) \cdot (JF)$$

Tables of properties (or the best estimates of properties) for possible alloy systems were prepared from the available literature. The numerical assignment of values to the importance of the various factor was accomplished as a team project by Dr. E. Thompson, Dr. F. Lemkey and Dr. C. Hulse of UTRC and Prof. H. Nowotny of the Univ. of Conn. Property factors based on estimated data were enclosed in parentheses and final rankings which involved more than two estimated properties were also enclosed in parentheses. The ten systems which obtained the highest rankings as a result of this initial effort are presented in Table II. Also indicated are the final six alloy systems selected for further work by the NASA Project Manager after further discussion and review at NASA Lewis.

The Pt-Pd-Mo system obtained the highest ranking primarily because of its low value of TCR and because it was the final recommendation as the best potential alloy by Bertodo after his extensive examination of many different alloy systems (Reference 7). The Pd-Ag-Mo system obtained the second highest ranking because of the very low values of TCR reported for the Pd-Ag system and because, it was felt, the further addition of Mo would lower the TCR even further and increase the resistivity up to acceptable levels. The Pt-10W and the FeCrAl systems were included in the final selected group despite their initially lower rankings as potential candidates primarily because there was a considerable background of experience with compositions in these systems and it was felt several systems of lower risk should be included.

The time during which the resistance data were being obtained in this program also coincided with continuing improvements being made in our electrical resistance measurement and control system. Although specific tests were not made to evaluate and develop numerical measures of potential errors, the accuracy of the data was being improved as the testing programs continued from lower to higher sample numbers. There were no standard reference materials which could be thermally cycled in our equipment to directly evaluate the behavior of our measurement system. These considerations apply most directly to the property measurements in the FeCrAl system which were the most extensive and carried out over the longest span of time.

The above comments are most relevant to our tests of cycle reproducibility and measurements of drift in electrical resistance over 3 hour periods at 1250K. In the cycle reproducibility testing, samples were heated and cooled at 10K/min and at 250K/min and the differences in resistance values at the end point in the different cycles noted at room temperature and at 1250K. In these tests and in the drift testing we estimate that the errors, which also include effects due to temperature measurement and furnace control, were reduced from approximately 500 $\mu\Omega/\Omega$ to $\pm$ 50 $\mu\Omega/\Omega$ as the program continued. We believe that the measurements were sufficiently accurate to make the necessary relative comparison between alloys.

The results of the experimental measurements in the subsequent Tables IV, VI, VIII and X should be considered relative to the program goals which are to obtain measurement accuracies equal to or better than 10 percent of full scale for strains up to ± 2,000 microstrain. Thus, at ± 2,000 microstrain an error greater than ± 200 microstrain from all sources would exceed the goal of the program. For a gage factor of 2.0, this would correspond to a change in electrical resistivity of ± 400 $\mu\Omega/\Omega$ from all effects not caused by strain of the alloy which could be accounted for by an apparent strain versus temperature correction curve. Typical temperature measurement uncertainties inside a gas turbine engine are approximately ± 15K.

The elastic and plastic strain capability data presented in these same tables were taken from stress versus strain curves obtained at room temperature and at 1250K. The compositions of the drop cast rod used for these measurements are indicated in the tables. The elastic strain limit was taken as the maximum strain before the initial part of the stress/strain curves become nonlinear. The microstrain reported as ε_{total} was the strain at failure.

5.3 Pt-Pd-Mo Alloys

The compositions and the sample numbers of the different Pt-Pd-Mo type alloys which were made and evaluated in this program are given in Table III. In the various systems studied, modification numbers refer to the various batch compositions examined. The sample numbers refer to specific samples made. These numbers will be the same unless more than one sample was made of the same composition. A general summary of the properties measured is presented in Table IV.

The change in $\Delta R/R$ for Modification #1 of this type versus temperature at 10K/min and 250K/min is shown in Figure 3. This was the composition recommended by Bertodo (Reference 7). This alloy was not subjected to a high temperature stabilizer heat treatment because of the extremely low rates of diffusion calculated for Mo even at extremely high temperatures. Electron microprobe measurements indicated that the composition was uniform within the ability of the electron beam to detect differences. The curves in Figure 3 indicate that this material does not behave in the desired linear or reproducible manner.

Figure 4 shows the $\Delta R/R$ versus temperature behavior of Modification #4 which showed better reproducibility and a lower TCR. Figure 5 shows the drift of this alloy composition over a 3 hr. period in argon at 1250K. A transvese section through the surface of a sample of Modification #4 after 50 hr. in static air at 1250K is shown in Figure 6. The depth of oxidation attack is of the order of 60 microns.

5.4 Pd-Ag-Mo and Nicrosil

Examinations of arc-melted pads of Pd-Ag-Mo revealed globules of silver which had not dissolved in the rest of the melt. Additional work on this alloy system was discontinued after further experiments confirmed this lack of solubility.

Measurements of the resistivities of Nicrosil versus temperature showed nonlinear behavior versus temperature and relatively high TCR's. These results were confirmed in similar measurements made at NASA-Lewis. In view of these results, it was decided to discontinue further work on this system in favor of the other candidates.

5.5 Pd-Cr Alloys

The compositions and the sample number of the six different Pd-Cr alloys which were examined in this program are presented in Table V. A general summary of the properties obtained is given in Table VI.

The change of $\Delta R/R$ for Pd-Cr alloy Modification #2 (Pd-13Cr) as a function of temperature is shown in Figure 7. The behavior is very linear which indicates that this microstructure is very stable. The resistivity increase of about 15 percent for this alloy when heated to about 1250K is very much greater than that observed for FeCrAl Modification #3 shown in Figure 8. The drift in resistance of this alloy over a 3 hr. period at 1250K in argon shown in Figure 8 was, however, very small. Figure 9 shows in cross-section the continuous oxide film which formed on the surface of this oxide during a 50 hr. exposure to air at 1250K.

5.6 Pt-W Alloys

The compositions and the sample numbers of the six different Pt-W type alloys which were made and examined in this program are given in Table VII. A general summary of the properties obtained are presented in Table VIII.

The change in $\Delta R/R$ for Modification #3 of this type alloy versus temperature at 10K/min and 250K/min is shown in Figure 10. This material does not appear to be sensitive to the rate of heating and cooling but some problems with reproducibility are indicated. Some change in behavior appears to be taking place above about 1200K. The $\Delta R/R$ versus temperature for the alloy judged to be the best, Modification #5, Pt-6.5W-6.5Re, is shown in Figure 11. This alloy shows linear behavior with temperature with only a slight indication that there might be a change occurring at the highest temperatures. The drift in the resistance of this alloy over a 3 hr. period at 1250K in argon is shown in Figure 12.

Figure 13 shows a transverse section of alloy Modification #5 after a 50 hr. exposure to static air at 1250K. The grain boundaries appear to have provided channels for the rapid diffusion of oxygen into the alloy. Figure 14 presents a Scanning Electron Microscope picture of the as oxidized surface of this alloy. It's surface has become faceted and contains many holes.

5.7 FeCrAl Alloys

Fourteen different FeCrAl alloy samples were prepared of 10 different compositions. Table IX lists the compositions examined. A general summary of the data obtained is given in Table X.

The various samples of this alloy type showed a wide variety of resistance versus temperature behaviors. Figures 15 through 19 show some of these curves for different compositions at different rates of heating and cooling. The least thermally sensitive composition, shown in Figure 18, was modification #3, Fe-10.6Cr-11.9 Al. Figure 20 shows a plot of the very low drift in resistivity that was observed for this sample over a three hour period in argon at 1250K.

Figure 21 shows curves of the changes in weight of some FeCrAl compositions over a 50 hour period in static air at 1250K. Alloy modification #3 was the only one, together with that of the Commercial Kanthal A-1 composition, which showed a positive weight gain with time. The other samples had more metallic, cleaner appearing surfaces which indicated that their oxide coatings were not as adherent. All of these samples experienced some thermal shock when they were suddenly removed from the furnace, in order to make room temperature weight measurements, and then again when they were suddenly replaced in the furnace. This thermal shocking may have encouraged spallation. Figure 22 shows a transverse view of the continuous oxide coating formed on the modification #3 oxidation sample. The typical depth of oxidation attack was about 2 microns with a maximum penetration in certain places of about 13 microns.

Figure 23 shows the thermal expansion of a sample of the same composition in air. Two cycles in air were run prior to the one shown in Figure 23 in order to stabilize the system and confirm reproducibility.

5.8 Sputtered Alloy Samples

In order to carry out the third part of the test plan, alloys of two different FeCrAl compositions were prepared as resistor networks by sputtering on alumina substrates. The purpose of this effort was to demonstrate that for well-annealed and stabilized materials of the same compositions, the same electrical properties would be obtained for samples prepared using the sputtering technique as for those prepared by casting directly from the melt.

The desired "corn cob" structure of an as-sputtered film of Fe-22.0Cr-5.7Al-0.5Co (Kanthal A-1) is shown in the Scanning Electron Microscope photo of Figure 24. The vague square in the upper picture was the result of an electron microprobe composition scan. The composition of the sputtered film was the same as that used to cast the target. Two of these samples were subsequently annealed and homogenized by heating for 3 hrs. in an argon atmosphere at 1473K. During this heat treatment, which was done in a furnace with a carbon resistor element, the samples were held inside an alumina tube which was wrapped in a Ta foil.

Attempts to measure the change in resistivity with temperature of one of these annealed samples at 50K/min in our tube furnace system purged with the building argon supply were not satisfactory. Although the purity of this argon was not measured, it was subsequently learned that it was variable because the line contained residual water from a plumbing accident. The resistance increased erratically until finally the sample would no longer conduct current. The change in the appearance of the sputtered surface is also shown in Figure 24. The film contains obvious cracks and has apparently undergone a significant amount of oxidation. Electron microprobe examinations also indicated that the composition of the surface was no longer as uniform as in the as-sputtered state. The amount of variation was not determined. Chromium especially had segregated into discrete modules. This process may have occurred primarily during the heat treatment at 1473K.

A second resistance measurement conducted using tank argon (purity approximately 1 to 2 ppm) introduced at one end of the heater tube gave only slightly better results. As a consequence of this oxidation, the thicknesses of the sputtered film was increased from 1.3 microns to 1.6 microns. The measured thicknesses of the oxidized materials were sharply greater just at the edges of the sputtered strips. This may have been caused by the volume increase resulting from oxidation.

5.9 Mechanical Properties

The mechanical properties of different alloys prepared by drop casting are presented in Table XI. The Pt-Pd-Mo Mod. 4 samples were too brittle and weak to test. An attempt to test this alloy at 1250K was terminated when the sample broke during heating because it was too weak to support even a small preload. Short time creep data at 1250K for different alloys is also presented in Table XI. Because of its' low strength, no attempts were made to obtain creep data for Pt-Pd-Mo Mod. 4.

6.0 DISCUSSION OF RESULTS

A comparison of the final best candidate alloys of the four different alloy types with their rankings at several different times during the program and a breakdown of their various final property scores is presented in Table XII. Since rankings decreased with increasing knowledge of the alloy properties, it follows that the alloys were not as good as we had guessed that they were. A major reason for the changes which lowered the ranking of the Pt-W and the Pt-Pd-Mo type alloys was the observation of appreciable internal oxidation attack in these systems. Comparisons of the depths of oxide attack in these alloys is presented in Table XIII together with some other properties of interest. These penetration distances are significantly deep so that, even if a grid of fine wires were used to make the sensor, serious changes in overall composition with time would be expected. The top candidate, Pd-Cr did better partly because it forms a protective oxide coating of Cr_2O_3. Thus, even in the case of a precious metal alloy, the formation of a stable oxide coating appears to be a reasonable requirement of a good alloy candidate.

The measures of reproducibility given in columns 3 and 4 of Tables IV, VI, VIII and X refer to the ability of these materials to return to the same values of the resistivity after heating and cooling that they had originally. These numbers also reflect some inaccuracies in our measuring system so that great emhasis should not be placed on their absolute values. The measurement system was quite able, we feel, to compare the behavior of different alloys to identify optimum candidates. Although no definitive determinations of accuracy were made, primarily because no standard reference materials were available, we believe our measurement accuracies were improved from about ± 500 $\mu\Omega/\Omega$ to about 50 $\mu\Omega/\Omega$ as the program progressed.

The resistance versus temperature curves for the FeCrAl type alloys, Figures 15 through 19, show marked variations which indicate a high sensitivity to composition. The equilibrium phase diagram (Reference 17) indicates that we should be in a single phase, solid solution area field. Naohara et. al. (References 18 and 19) have described a variety of effects that can occur when rapidly quenched alloys of these types are heated. Although the reasons for our observations of nonlinear behavior were not determined, they probably are due to a series of relatively high speed ordering effects, some of which may be opposing each other, which occur over a range of temperatures. These effects are probably also the reason for the change in slope of the thermal expansion curve which occurs at about 700K (Figure 23).

Figure 25 shows where some of these compositions occur on the ternary phase diagram and defines an area inside of which the TCR's from room temperature to 1250K have net negative values. Compositions which lie at the edges of this area

will have average TCR's of zero. It is these compositions which are of most interest, if they are the most reproducible, stable, and show relatively linear changes in resistivity with temperature.

A comparison of the behavior of the FeCrAl Modification #3 alloy with that of Kanthal A-1 after a pretreatment of 2 Hr. at 1153K is shown in Figure 26. The Kanthal A-1 data were obtained from our prior work (Reference 4). The newer alloy of Fe-10.6 Cr-11.9 Al has a lower sensitivity to temperatures and a lower sensitivity to the rate of temperature change over a wider range of temperatures.

In regard to the results obtained with sputtered FeCrAl films in Section 5.8, the cracks in the films shown in Figure 24 may have been caused primarily by the requirement that the films accommodate the thermal expansion of the alumina substrate. Because the thermal expansion of Al_2O_3 is less than that of FeCrAl, we would expect the differential expansion forces on the metal film to have been primarily compressive during heating and that the film would go into tension upon cooling to create the cracks shown. If the film had been deposited on a nickel-based superalloy, especially one with a ductile interlayer, these cracks might not have formed.

The observation that the measured thicknesses of the oxidized materials were sharply greater just at the edges of the sputtered strips, suggests that the volumes of the oxides formed tend to be greater than that of the alloy from which they are formed. These volume differences may create stresses which would encourage spalling of the films.

It is also felt that if sputtered films are to be used as strain gages they should initially be much thicker than these films were in order to provide a sufficient amount of material to be consumed in forming a protective oxide coating. It was suspected that oxidation effects might also have been at least partly responsible for the nonlinear behavior in the data for the change in resistance versus temperature of precious metal alloys at higher temperatures.

The Pd-13 wt% Cr composition which was selected as the best alloy has the particular advantage that it is a relatively simple system which forms an adherent, protective oxide surface film of Cr_2O_3. Chromia is a very high melting oxide (2620 K) which, together with alumina, forms on nickel and cobalt base superalloys to provide them with the necessary corrosion resistance to function effectively inside gas turbine engines. The linear resistance versus temperature behavior observed, together with the very small amounts of electrical drift, indicates that the chromium remains in complete solid solution over the temperature range of interest and that internal time dependent ordering, exsolution or precipitation reactions do not occur. These factors support the view that this is a very stable system alloy system which should show good reproducibility when used as a strain gage element.

7.0 SUMMARY OF RESULTS

The available literature about strain gages and potential high temperature, alloy resistors was surveyed. A ranking system to evaluate various types of alloys was developed and used to select ten primary candidates. After further review at NASA, this list was reduced to six: 45Pt-45Pd-10Mo, 60Pd-30Ag-10Mo, Pd-30Cr, Pt-10W, Nicrosil and modifications near the Kanthal A-1 composition in the FeCrAl system.

Test samples were prepared by arc-melting followed by drop casting into ceramic tubes and then polishing the resultant rods into flat strips. An apparatus was developed which was capable of making measurements of resistivity at either constant temperatures or at cycle rates of from 50 to 250K/min from room temperatures to 1250K in a purged argon atmosphere. This resistance measurement facility was improved by the addition of a computer controlled data collection system during the latter part of the program.

The Pd-Ag-Mo system was eliminated as a candidate system when problems of liquid immiscibiity were encountered. The Nicrosil system was also dropped because of its relatively high thermal sensitivity of resistance and its nonlinear response to temperature. The best alloy discovered was Pd-13Cr (in weight percent) with Fe-10.6Cr-11.9Al a close second. The Pd-13 Cr alloy had a very linear increase of resistivity with temperature which indicates that no ordering or other temperature dependent microstructural changes were taking place within the temperature range of interest. The results from the drift in resistance and the oxidation measurements at 1250 K were also particularly good. Alloys of Pt-6.5W-6.5Re and 45Pt-45Pd-10Mo were ranked behind these two alloys primarily because of the much larger degree of oxide penetration attack they showed after 50 hours in static air at 1250K, typically 200 and 10 microns, respectively. The first and second place alloy candidates showed typical depths of oxidation attack of only about 2 microns.

Measurements of the electrical resistances of a 1.6 micron thick sputtered FeCrAl sample indicated that (a) some oxidation could still occur in our measurement system despite it's being continually purged with argon, and (b) oxidation can be a serious problem for such thin films. If the sputtering technique is to be used to prepare strain gages, they should be made of appreciable thickness.

Although many alloys were prepared and examined, additional work is advisable in order to confirm these results with more accurate $\Delta R/R$ measurements and to optimize the properties of these alloys with ternary and higher element additions.

8.0 REFERENCES

1. Stetson, K; and Grant, H.: Burner Liner Strain Measurement, Contract NAS3-2369, United Technologies Research Center.

2. Lemcoe, M. M.: Development of High-Temperature Strain Gages, NASA CR-112241, 1973.

3. Lemcoe, M. M.: Development of Strain Gages for Use to 1311 K (1900F), NASA CR-132485, 1974.

4. Hulse, C.; Stetson, K.; Grant, H.; Jameikis, S.; Morey, W.; Raymondo, P.; Grudkowski, T.; and Bailey, R.: Advanced High Temperature Static Strain Sensor Development Program, NASA Contract NAS3-22126 at United Technologies Research Center, Final Report in Progress.

5. Bertodo, R: Resistance Strain Gages for the Measurement of Steady Strains a Temperature above 650°C, Journal of Strain Analysis, Vol. 1, No. 1, 1965, pp. 11-19.

6. Bertodo, R.: High Temperature Strain Gages for Turbo-Jet Components, Platinum Metals Review, Vol, 8, No. 4, 1964, pp. 128-130.

7. Bertodo, R.: Resistances Strain Gauges for the Measurement of Steady Strains at High Temperatures, Proc. Inst. Mech. Engrs., Vol. 178, Pt. 1, No. 34, 1963-64, pp. 907-926.

8. Bertodo, R.: Platinum Metal Alloys for the Measurement of Strains at High Temperatures Englehard Industries Tech. Bulletin, Vol. 9, No. 2, 1968, pp. 37-49.

9. Easterling, K.: High Temperature Resistance Strain Gauges, Brit. J. Appl. Phys., Sem. 2, Vol. 1, 1968, pp. 1743-52.

10. Easterling K.: High Temperature Resistance Strain Gauges, Brit. J. Appl. Phys., Vol. 14, 1963, pp. 79-84.

11. ASTM Special Technical Publication No. 230, Symposium on Eleveated Temperature Strain Gages, ASTM, 1957.

12. Graft, W.: Development of High-Temperature Strain Gage Wire, ASTM STP 230, 1957, pp. 76-86.

8.0 REFERENCES (Cont'd)

13. Weise, R.; and Foster, J.: High Temperature Strain Gage System for Application to Turbine Engine Components, Technical Report AFWAL-TR-80-2126, Wright-Patterson, 1980.

14. Zhi-qi; and Pei-quig, H.: Development of the Self-Temperature Compensated Resistance Strain Gage used up to 700 C, ASME Paper 81-GT-118, 1981.

15. Wu, Tsen-tai, et al.: Development of Temperature-Compensated Resistance Strain Gages for Use to 700°C, Exp. Mech., Vol. 21, No. 3, 1981, pp. 117-123.

16. Mooij, J.: Electrical Conduction in Concentrated Disordered Transition Metal Alloys, Phys. State Sol. (a) Vol. 17, 1973, p. 521.

17. Rivlin, V.; and Raynor, G.: Critical Evaluation of Aluminum-Chromium-Iron System, International Metals Review, No. 4, 1980, pp. 139-157.

18. Naohara, T.; Noue, A. I.; Minemura, T.; Masumoto, T.; and Komada, K.: Microstructures, Mechanical Properties and Electrical Resistivity of Rapidly Quenched Fe-Cr-Al Alloys, Metallurgical Transactions A, Vol. 13 A, 1982, pp. 337-343.

19. Naohara, T.; Noue, A. I.; Masumoto, T.; and Kumada, K.: Mechanical Properties and Electrical Resistivity of Melt-Quenched Fe-Cr-Al and Fe-Cr-Al-M (M = IV and V Group Transition Metals) Alloys, Proc. 4th Int. Conf. on Rapidly Quenched Metals, Sendai, 1981, pp. 1581-1584.

TABLE I

ALLOY EVALUATION FACTORS

Property	Symbol	Value Range
Repeatable Resistance (structural stability)	R_p	1-20
Oxidation Resistance	0	1-18
Resistivity	ρ	1-16
Temperature Coefficient of Resistivity	TCR	1-14
Elastic Range	$\Delta\epsilon$	1-12
Thermal Expansion Match to Superalloys	$\Delta\alpha$	1-10
Judgement Factor	J.F.	1-10

TABLE II

BEST ALLOY CANDIDATES

Alloy	Ranking Score x 10^5	NASA Approved
45 Pt-45 Pd-10 Mo	148	yes
60 Pd-30 Ag-10 Mo	(118)	yes
Nicrosil	111	yes
Pd-20 Mo	97	no
Pd-30 Cr	94	yes
Pd-12 W	83	no
60 Pd-30 Au-10 Mo	79	no
Pt-10 W	58	yes
Pt-15 Mo	51	no
Modified FeCrAl	47	yes

TABLE III

THE COMPOSITIONS OF ALLOYS OF THE Pt-Pd-Mo TYPE IN WEIGHT PERCENT

Element	Modification Number				
	#1	#2	#3	#4	#5
Pt	45	43	40	48	48
Pd	45	43	48	40	40
Mo	10	14	12	12	6
W	–	–	–	–	6
Sample Number	PtPdMo-1 -2 -3	-4	-6	-5	-7

TABLE IV

PROPERTIES OF PLATINUM-PALLADIUM-MOLYBDENUM ALLOY CANDIDATES

| Sample # | Mod. # | Cycle Reproducibility 10K/min vs 250K/min ΔμΩ/Ω | | Avg. TCR (μΩ/Ω/K) R.T. to 1250K | Drift (μΩ/Ω/Hr) 1250K | Oxidation ΔW(mg/cm²) 50 Hrs, Static Air, 1250K | ρ (μΩ-cm) R. Temp. | Strain Capability (με) | | Thermal Expansion (μm/m/K) |
		R.T.	1250					ε_{Total} RT/1250	$\varepsilon_{Elastic}$ RT/1250	
PtPdMo-1	1	-	-	+83	-	-	22.6	-	-	-
PtPdMo-2	1	-	-	+86	-	-	-	-	-	-
PtPdMo-3	1	1,100	2,300	+222	+1,700	-	101	-	-	-
PtPdMo-4	2	0	4,890	+165	+1,750	-	148	-	-	-
PtPdMo-5	4	8,300	3,130	+81	-1,600	-1.50	-	-	-	9.7
PtPdMo-6	3	13,300	9,500	94	-225	-	73	-	-	-
PtPdMo-7	5	7,100	4,200	113	-5,600	-	-	-	-	-

TABLE V

THE COMPOSITIONS OF STRAIN GAGE ALLOYS OF THE Pd-Cr
TYPE IN WEIGHT PERCENT

Element	Modification Number					
	#1	#2	#3	#4	#5	#6
Pd	82.7	87	74	84	78	78
Cr	17.3	13	13	12	13	13
Mo	-	-	13	-	9	-
Co	-	-	-	4	-	-
Wa	-	-	-	-	-	4.5
Ta	-	-	-	-	-	4.5
Sample Number	PdCr-1	-2	-3	-4	-5	-6
		-9			-7	-8

TABLE VI

PROPERTIES OF PALLADIUM-CHROMIUM ALLOY CANDIDATES

Sample #	Mod. #	Cycle Reproducibility 10K/min vs 250K/min ΔμΩ/Ω		Avg. TCR ($\mu\Omega/\Omega/K$) R.T. to 1250K	Drift ($\mu\Omega/\Omega/Hr$) 1250K	Oxidation $\Delta W(mg/cm^2)$ 50 Hrs, Static Air, 1250K	ρ ($\mu\Omega$-cm) R. Temp.	Strain Capability ($\mu\varepsilon$)		Thermal Expansion ($\mu m/m/K$)
		R.T.	1250					ε_{Total} RT/1250	$\varepsilon_{Elastic}$ RT/1250	
PdCr-1	1	1,557	28,970	+153	+837	–	51	250,000	740/332	13.8
PdCr-2	2	2,700	1,900	+153	~0	+.59	82	30,000		
PdCr-3	3	1,100	21,700	+232	+6,100	–	7(?)			
PdCr-4	4	4,596	2,480	+175	+2,910	–				
PdCr-7	5	6,529	7,700	133	8,800					
PdCr-8	6	18,300	6,500	128	4,770	–	73			

TABLE VII

THE COMPOSITIONS OF STRAIN GAGE ALLOYS OF THE Pt-W
TYPE IN WEIGHT PERCENT

Element	Modification and Sample Number #1	#2	#3	#4	#5	#6
Pt	90.52	78	84	87	87	87
W	9.48	22	16	13	6.5	6.5
Re	-	-	-	-	6.5	-
Ta	-	-	-	-	-	6.5

TABLE VIII

PROPERTIES OF PRECIOUS METAL STRAIN GAGE ALLOY CANDIDATES

Platinum-Tungsten

Sample #	Mod. #	Cycle Reproducibility 10K/min vs 250K/min $\Delta\mu\Omega/\Omega$		Avg. TCR $(\mu\Omega/\Omega/K)$ R.T. to 1250K	Drift $(\mu\Omega/\Omega/Hr)$ 1250K	Oxidation $\Delta W(mg/cm^2)$ 50 Hrs, Static Air, 1250K	ρ $(\mu\Omega\text{-cm})$ R. Temp	Strain Capability $(\mu\varepsilon)$		Thermal Expansion $(\mu m/m/K)$
		R.T.	1250					$\varepsilon_{Elastic}$ RT/1250	ε_{Total} RT/1250	
PtW-1	1	5,360	1,590	+171	+656 in 1st 10 min		63			+8.4
PtW-2	2	5,714	31,600	+ 45	+2,206		132			
PtW-3	3	4,310	3,980	+ 60	+1,598		112			
PtW-4	4	4,750	3,160	+114	1,783		119			
PtW-5	5	7,300	4,440	+102	+179	-1.00		1,053/ 560	160,000/ 64,000	+9.5
PtW-6	6	47,186	97,420	+278	-6,980					

TABLE IX

THE COMPOSITIONS OF STRAIN GAGE ALLOYS OF THE FeCrAl TYPE IN WEIGHT PERCENT

Element						Modification Number					
	#1	#2	#3	#4	#5	#6	#7	#8	#9	#10	A-1
Fe	77	72.5	77.5	72	75.0	72.0	68.0	77.0	77.5	63	71.8
Cr	18	17	10.6	20	13.8	23.0	23.0	7.0	10.6	13	22.0
Al	15	10.5	11.9	8.0	11.2	15.0	19.0	16.0	11.9	24	5.7
Co	-	-	-	-	-	-	-	-	-	-	0.5
Sample Number	K-1 -2 -4	K-3 -7	K-5	K-6	K-9	K-10	K-11	K-12	K-13	K-14	K-8

TABLE X

PROPERTIES OF FeCrAl TYPE ALLOY CANDIDATES

Sample #	Mod. #	Cycle Reproducibility 10K/min vs 250K/min ΔμΩ/Ω R.T.	Cycle Reproducibility 1250	Avg. TCR (μΩ/Ω/K) R.T. to 1250K	Drift (μΩ/Ω/Hr) 1250K	Oxidation ΔW(mg/cm²) 50 Hrs, Static Air, 1250K	ρ μΩ-cm R.Temp.	Strain Capability (με) ε_{Total} RT/1250	$\varepsilon_{Elastic}$ RT/1250	Thermal Expansion (μm/m/K)
K-1	1	1,600	0	-60	+246	—	131			
K-2	1	0	3,140	-54	+181 in 1st 10 min.	—	139			
K-3	2	4,500	2,600	-40	+166	—	128			
K-4	1	12,200	0	-357	0	—	254			
K-5	3	3,800	3,480	-9	0	0.34	129	127,000	1,040	17.2
K-6	4	3,200	3,000	-137	+686	—	210	230,000	571	
K-7	2	1,370	1,370	-88	-83	—	159			
K-8	A-1	6,015	4,220	+36	+817	—	135			
K-9	5	3,937	7,750	+22	-556	—	204			
K-10	6	—	—	-111	—	—	244			
K-11	7	—	—	-216	—	—	255			
K-12	8	—	—	-30	—	—	187			
K-13	9	0	0	7	+1,160	—				
K-14	10	11,527	9,510	+166	+366	—				

TABLE XI

MECHANICAL PROPERTIES OF STRAIN GAGE ALLOYS IN AIR

Tensile Tests 0.005 cm/cm/min.

Alloy	Composition (wt. %)	Temp. (k)	Elastic Modulus (GPa)	Ultimate Tensile Strength (MPa)	Yield Strength (MPa)	Strain Elastic (µε)	Strain Total (µε)
FeCrAl-Mod #3	Fe-10.6Cr-11.9Al	R.T.	105	312	216	1040	127,000
		800	-	121	102	-	77,000
		1250	-	8.3	7.5	571	230,000
PdCr-Mod #2	Pd-13Cr	R.T.	134	265	79	740	250,000
		1250	-	20.2	17.8	332	30,000
PtW-Mod #5	Pt-6.5W-6.5Re	R.T.	219	433	231	1057	160,000
		1250	-	75.1	28.9	702	64,000
PtPdMo-Mod #4	Pt-40Pd-12Mo	R.T.	Broke at void during set-up				
		1250	Broke during heat up				

Creep Tests

Alloy	Temp. (K)	Stress (MPa)	Fraction of Yield Stress (%)	Time (Min)	Total Creep Strain (µε)
FeCrAl-Mod #3	1250	6.54	80	55	451,252
PdCr-Mod #2	1250	8.82	50	180	5,000
PtW-Mod #5	1250	14.5	50	180	1,650

TABLE XII

FINAL ALLOY SELECTION RESULTS

Alloy Type*	Final Scores							Preliminary Ranking**		Final Ranking**
	Rate and Drift Stability R (1-20)	Oxidation O (1-18)	Resistivity ρ (1-16)	TCR α (1-12)	Δε Elastic (1-12)	ΔCTE (1-10)	Judgement JF (1-10)	3/10/82	8/25/82	10/10/82
PdCr-Mod#2 Pd-13Cr	17	12	12	4	8	8	9	94.1×10^5	44.2×10^5	56.5×10^5
FeCrAl-Mod#3 Fe-11.9Al-10.6Cr	12	12	14	7	4	8	8	47.0×10^5	83.8×10^5	36.1×10^5
PtW-Mod#5 Pt-6.5W-6.5Re	15	5	14	8	10	4	5	57.6×10^5	42.6×10^5	16.1×10^5
PtPdMo-Mod#4 48Pt,40Pd,12Mo	8	3	14	6	9	4	5	148×10^5	145.6×10^5	3.6×10^5

* Numbers indicate weight percent
** Rank = (R) · (O) · (ρ) · (TCR) · (Δε) · (ΔCTE) · (JF)

TABLE XIII

NON-ELECTRICAL PROPERTIES OF SELECTED CANDIDATE STRAIN GAGE ALLOYS

Alloy	Melting Point (K)	CTE (ppm/K)	ΔCTE* from superalloy (ppm/K)	50 hrs in static air at 1250K		
				Wt change (mg/cm^2)	Oxide penetration (microns)	
					Typical	Maximum
Pd-Cr (Mod#2)	1670	13.8	-1.7	0.59	2	18
FeCrAl (Mod#3)	1818	17.2	+1.7	0.33	2	13
Pt-W (Mod#5)	2165	9.5	-6.0	-1.00	200	300
Pt-Pd-Mo (Mod#4)	>1985	9.7	-5.8	-1.50	10	64
Nicrosil	1710	14.3	-1.3	+0.97	-	-
Kanthal A-1	1780**	15.0	-0.5	+0.23	-	-

  * Typical TCE of superalloy 15.5 ppm/K, Al_2O_3=7 ppm/K
 ** Kanthal Corp. handbook
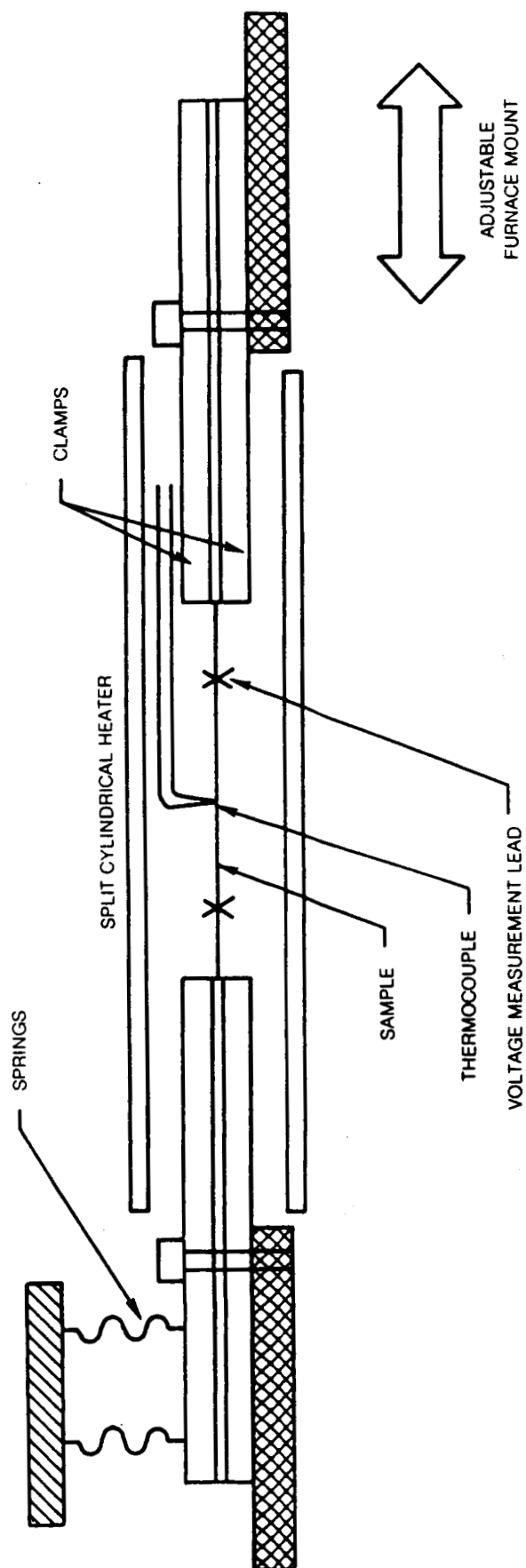
Figure 1. High-Speed Thermal Cycle/Resistivity Measurement Apparatus

ADJUSTABLE
FURNACE MOUNT

CLAMPS

SPLIT CYLINDRICAL HEATER

SPRINGS

SAMPLE

THERMOCOUPLE

VOLTAGE MEASUREMENT LEAD
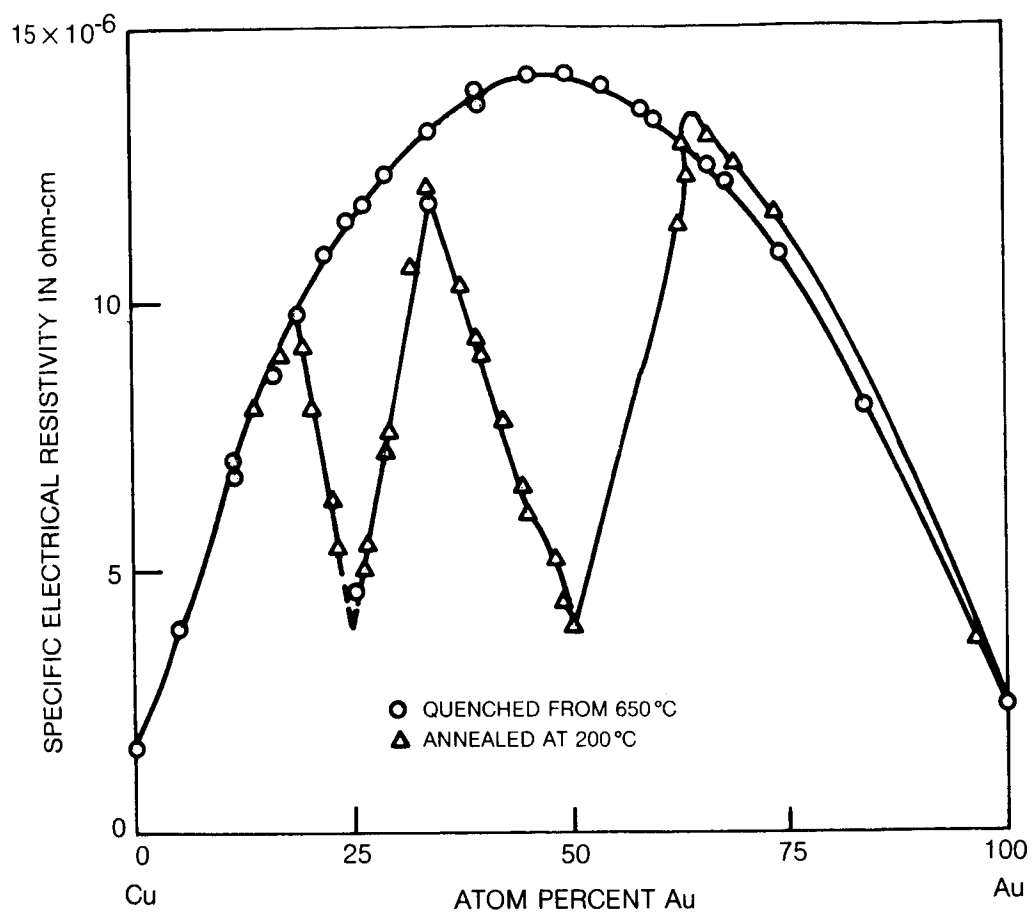
Figure 2. Effect of Alloying and Ordering on Electrical Resistivity in the Copper Gold System

(Pt-45Pd-10Mo, SAMPLE PtPdMo-3, AS CAST, PRESOAKED 20 min IN APPARATUS AT 1250K, EST. ERROR ± 100 ppm)
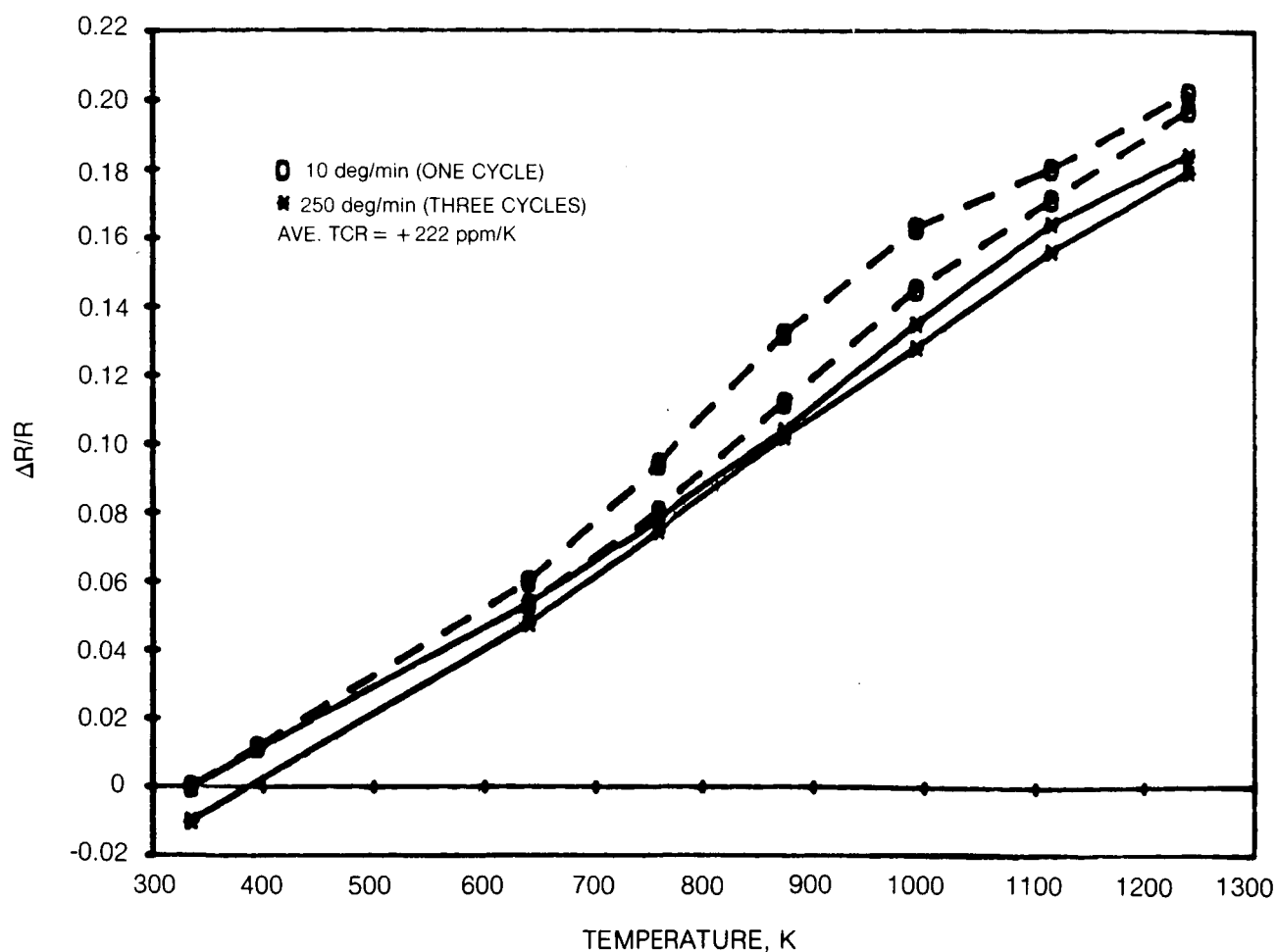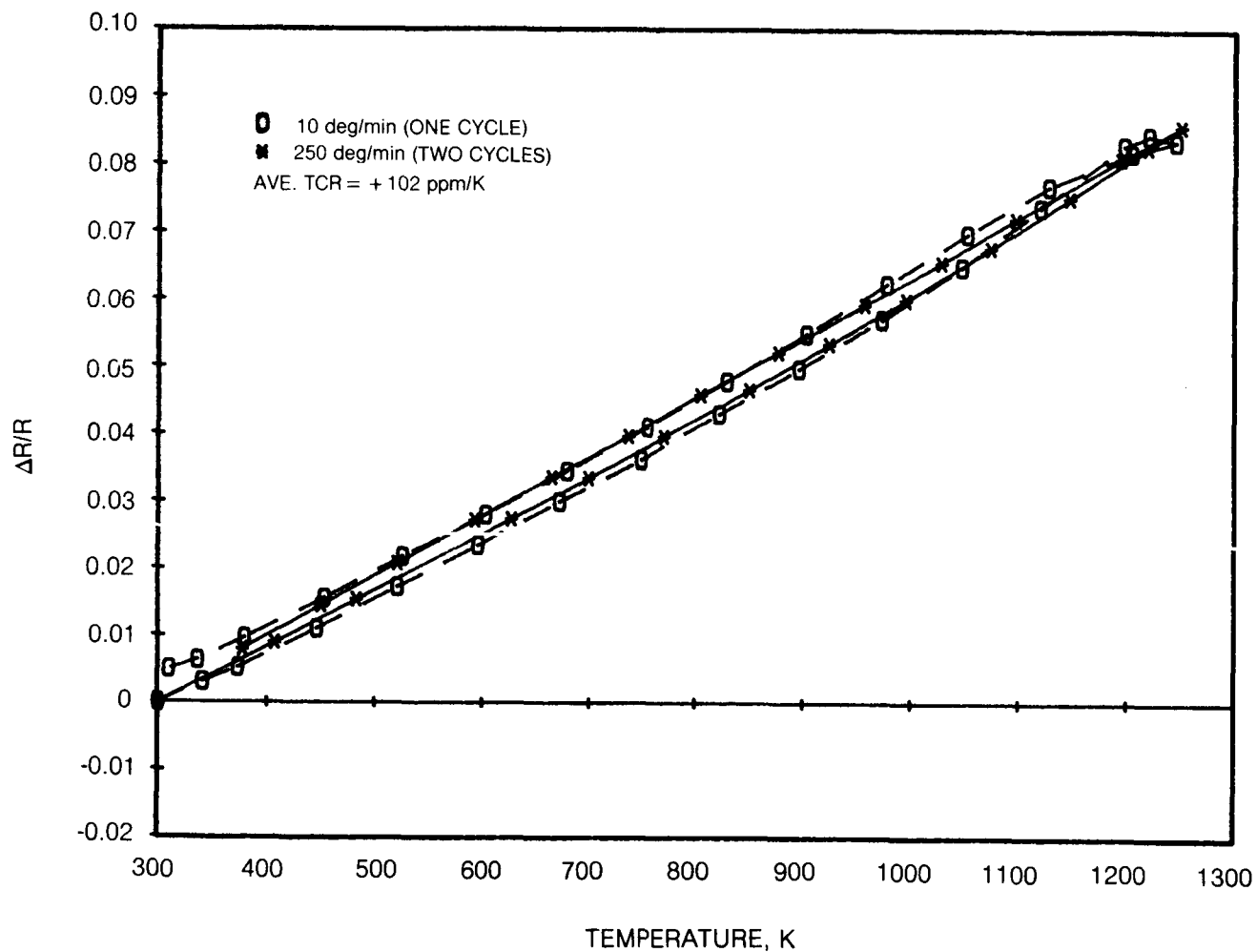

Figure 3. Change in Average Electrical Resistance vs Temperature of PtPdMo Mod #1 at Different Rates of Heating and Cooling

(Pt-40Pd-12Mo, SAMPLE PtPdMo-5, AS CAST, PRESOAKED 20 min IN APPARATUS AT 1250K, EST. ERROR ± 100 ppm)
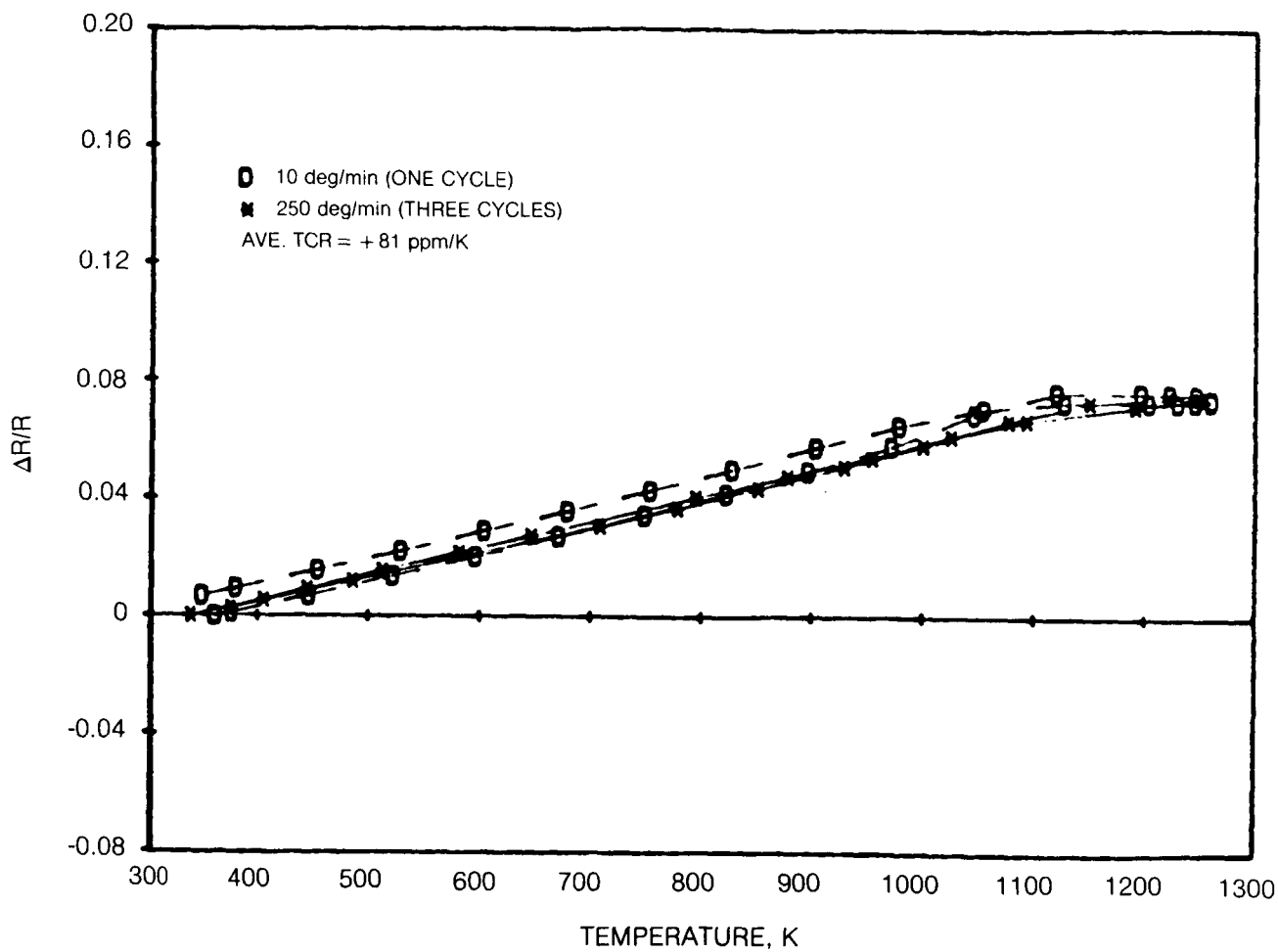

Figure 4. Change in Average Electrical Resistance vs Temperature of PtPdMo Mod #4 at Different Rates of Heating and Cooling

(Pt-40Pd-12Mo, SAMPLE PtPdMo-5, AS CAST, PRESOAKED 20 min. IN APPARATUS AT 1250 K, EST. ERROR ± 100 ppm)
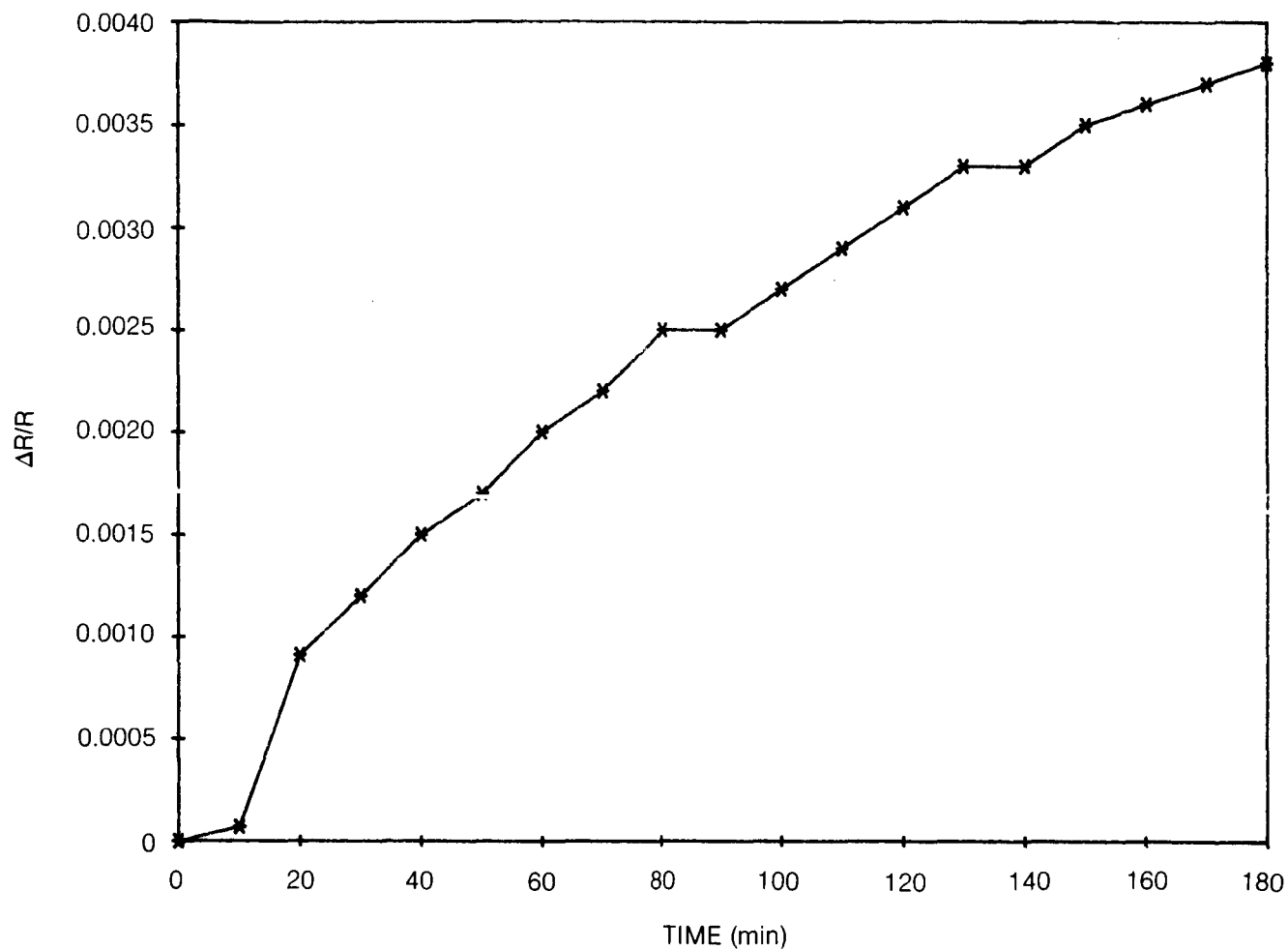
Figure 5. Electrical Resistance Drift of PtPdMo Mod #4 Over a 3 Hour Period at 1250K

AFTER 50 hrs, STATIC AIR, 1250 K

40μm
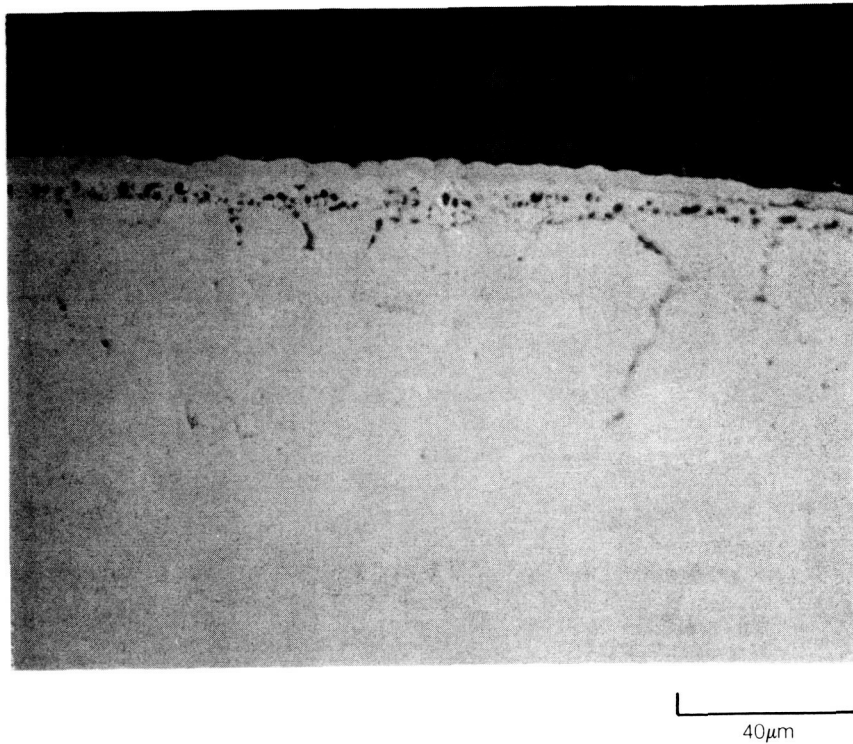
Figure 6. Transverse Section of Oxidized Surface of PtPdMo Mod #4, Pt-40Pd-12Mo

84–9–35–22

(Pd-13Cr, SAMPLE PdCr-9, AS CAST, PRESOAKED 20 min IN APPARATUS AT 1250K, EST. ERROR ± 50 ppm/K)
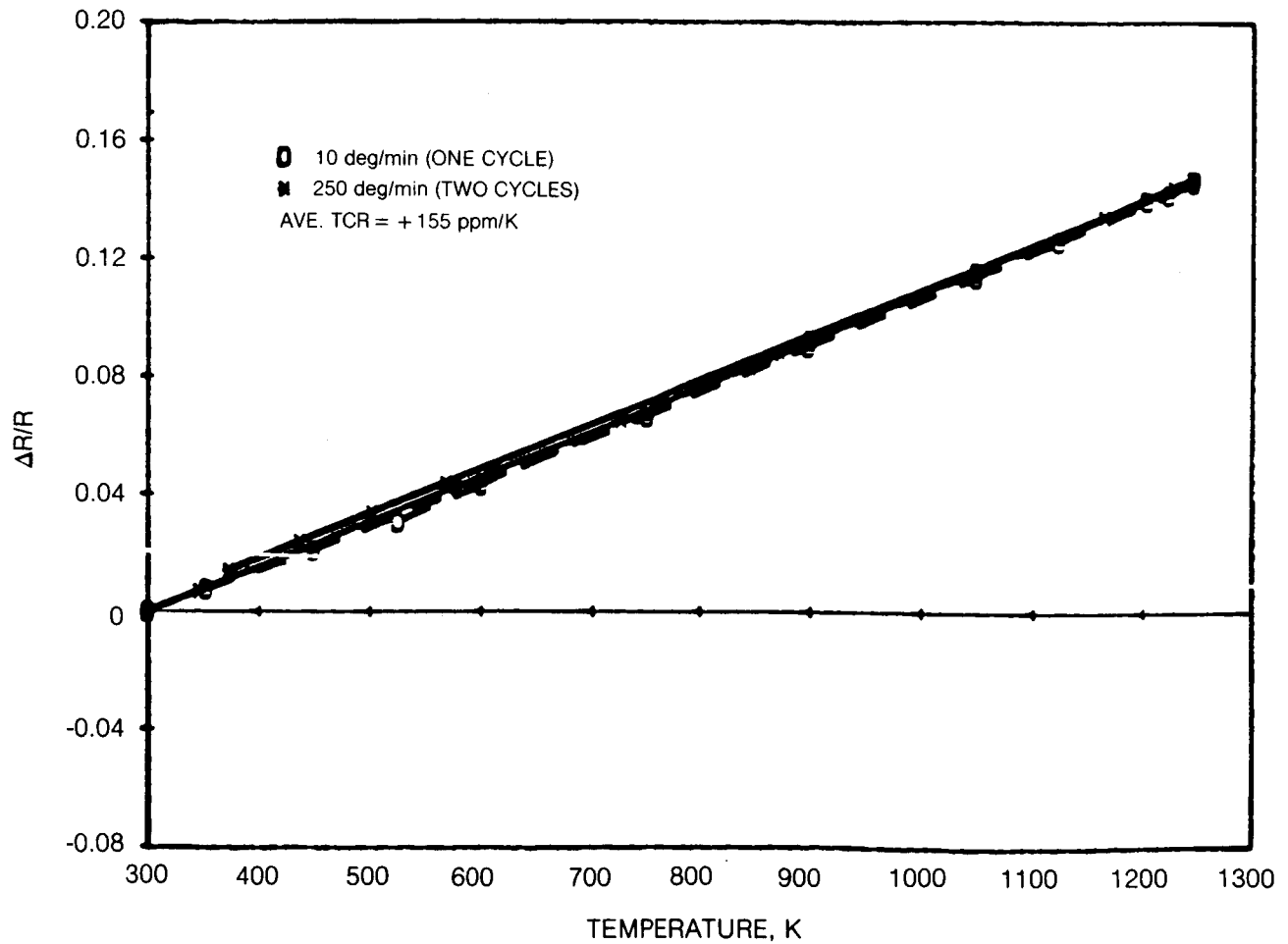
Figure 7. Change in Average Electrical Resistance vs Temperature of PdCr Mod #2 at Different Rates of Heating and Cooling

(Pd-13Cr, SAMPLE PdCr-9, AS CAST , PRESOAKED 20 min. IN APPARATUS AT 1250 K, EST. ERROR ± 50 ppm/K)
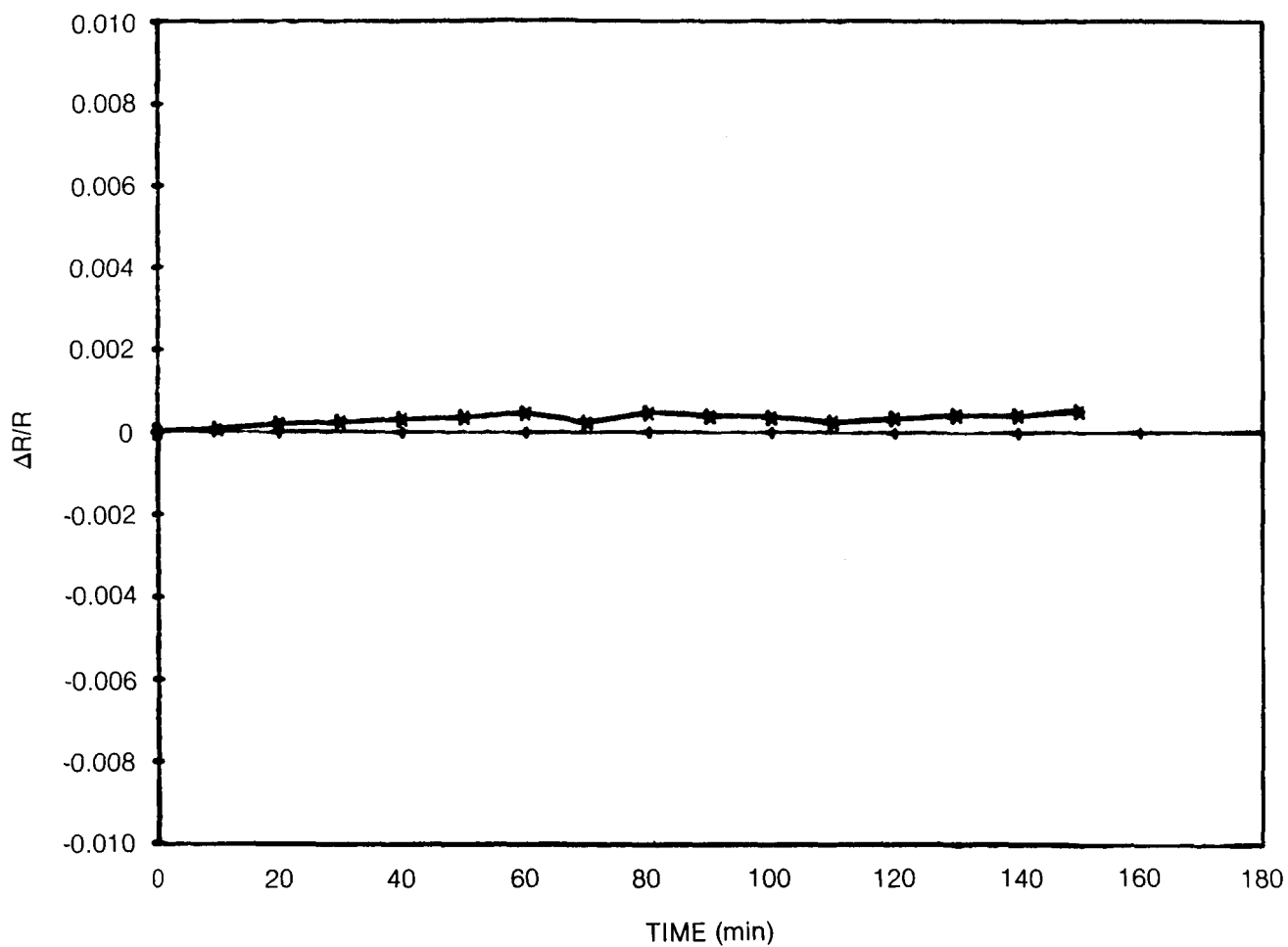
Figure 8. Electrical Resistance Drift of PdCr Mod #2 Over a 3 Hour Period at 1250 K in Air

AFTER 50 hrs, STATIC AIR, 1250 K

20μm
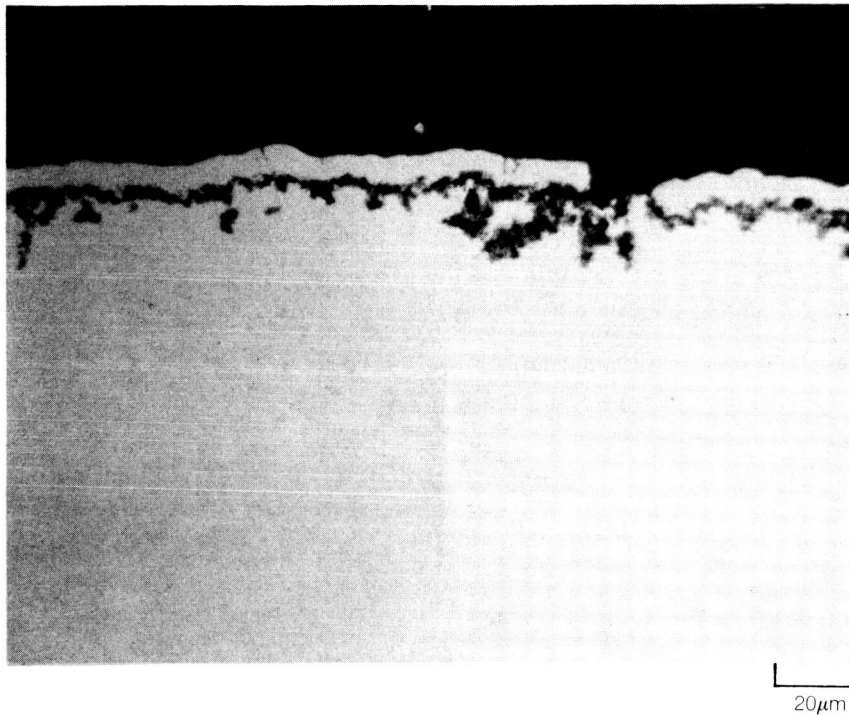
Figure 9. Transverse Section of Oxidized Surface of PdCr Mod #2, Pd-13Cr

84—9—35—13
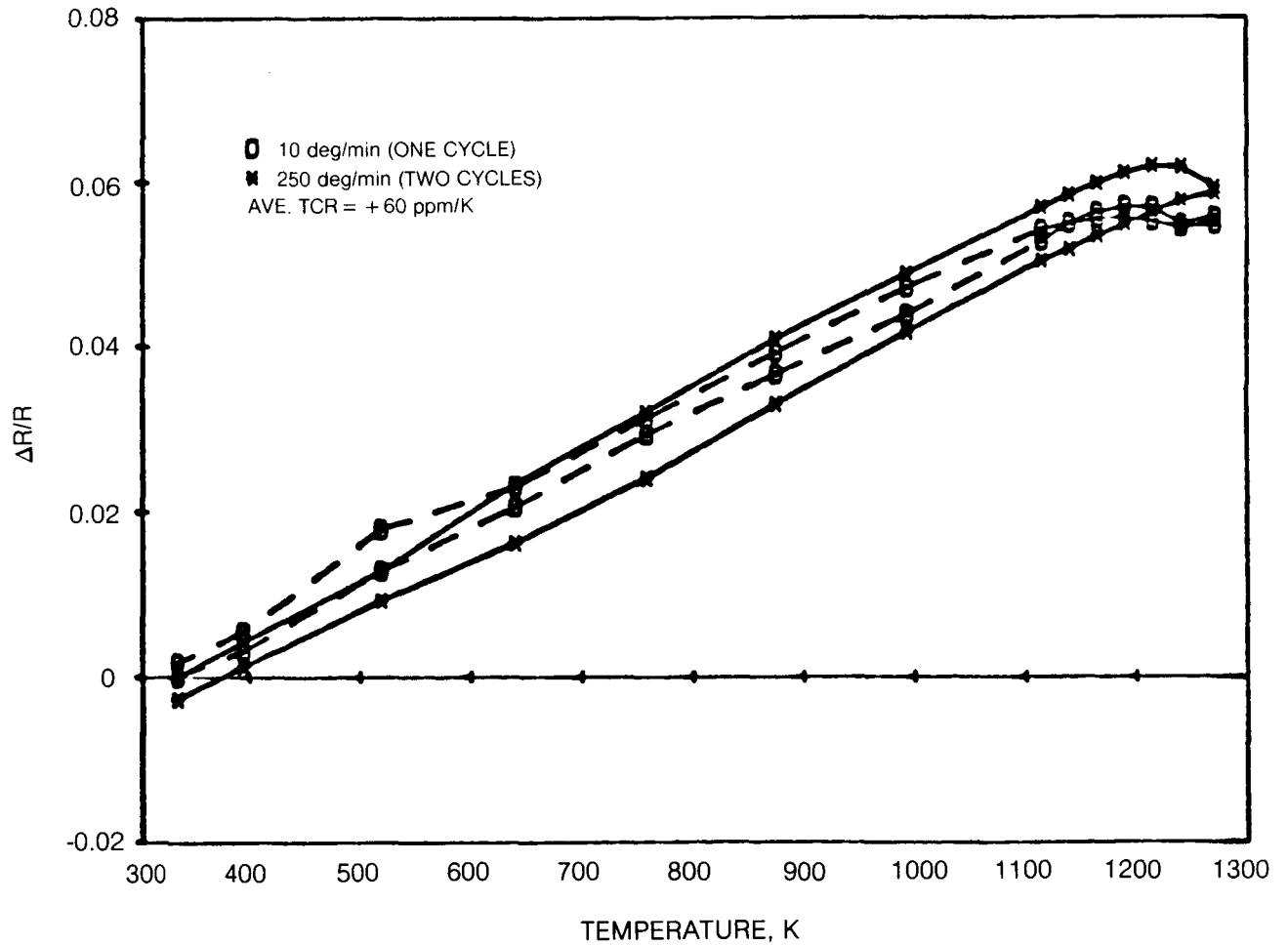
Figure 10. Change in Average Electrical Resistance vs Temperature of PtW, Mod #3 at Different Rates of Heating and Cooling

(Pt-6.5W-6.5Re, SAMPLE PtW-5, AS CAST, PRESOAKED 20 min IN APPARATUS AT 1250 K, EST. ERROR ±50 ppm)

Figure 11. Change in Average Electrical Resistance vs Temperature of PtW Mod #5
at Different Rates of Heating and Cooling
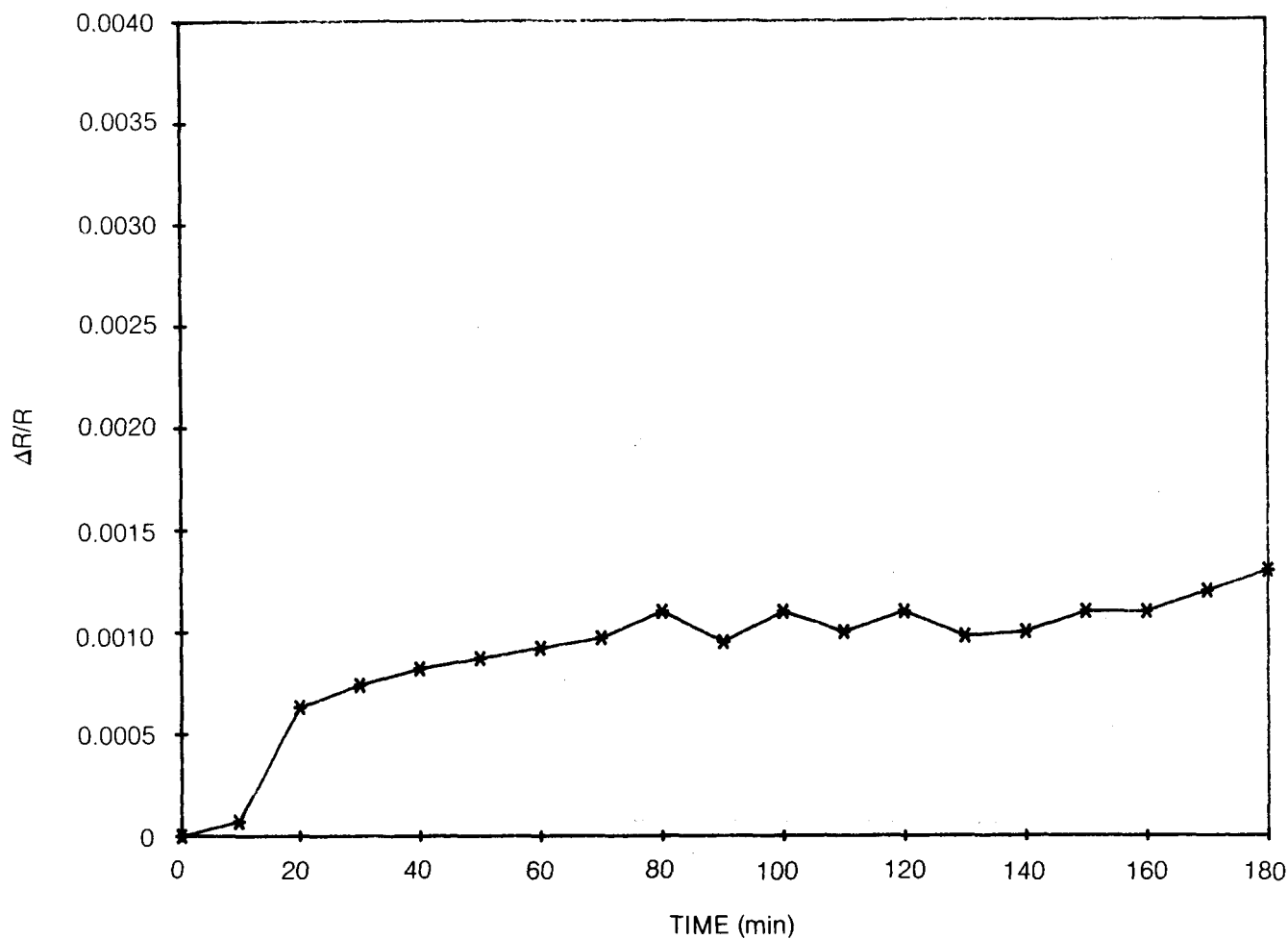
Figure 12. Electrical Resistance Drift of PtW Mod #5 Over a 3 Hour Period at 1250 K

AFTER 50 hrs, STATIC AIR, 1250 K

200μm
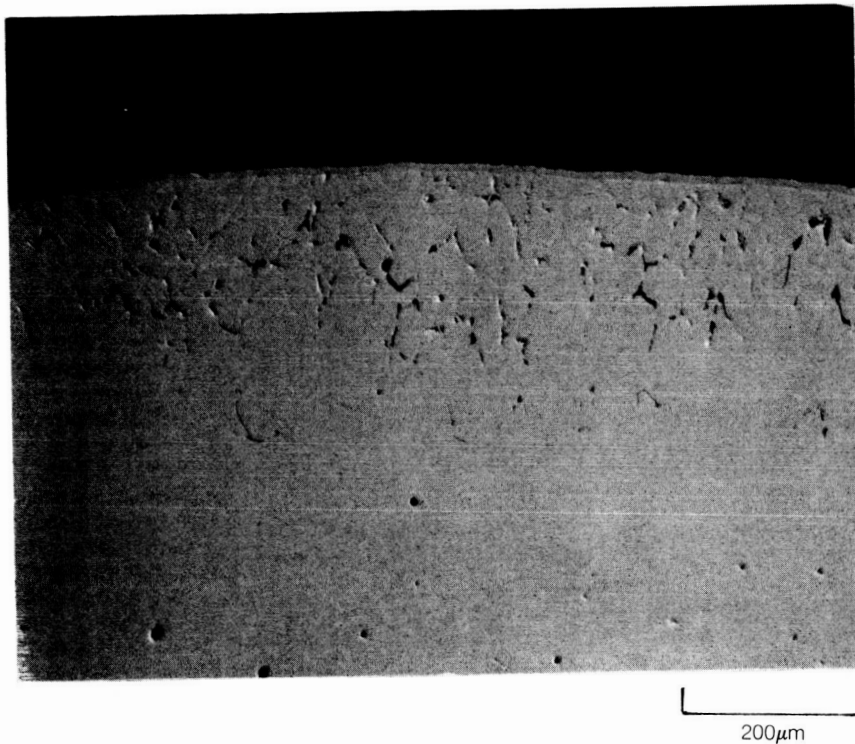
Figure 13. Transverse Section of Oxidized Surface of PtW Mod #5, Pt-6.5W-6.5Re

84—9—35—17

AFTER 50 hrs, STATIC AIR, 1250 K

5μm
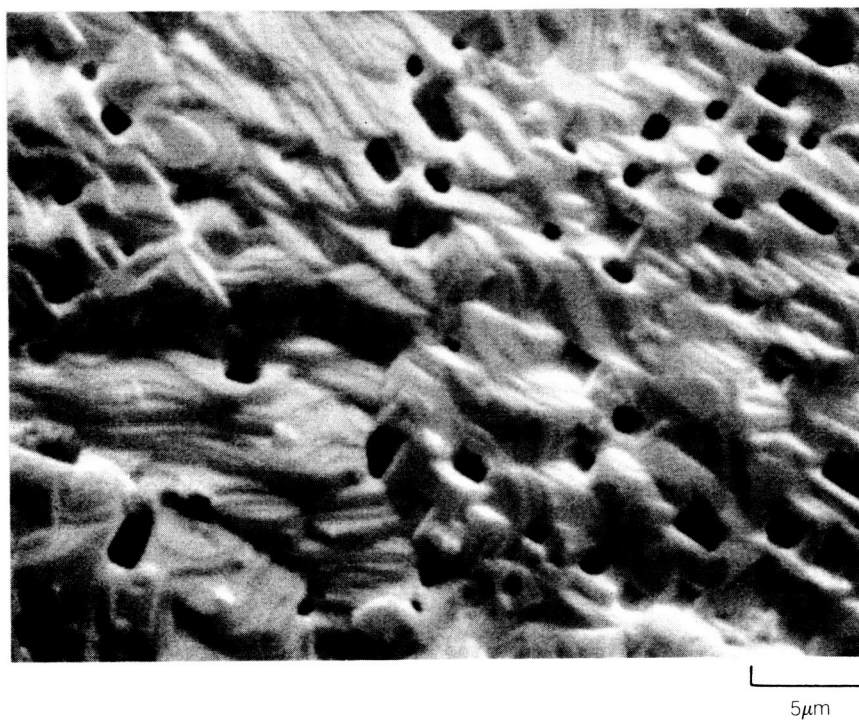
Figure 14. Oxidized Surface of Pt W Mod #5, Pt-6.5W-6.5Re
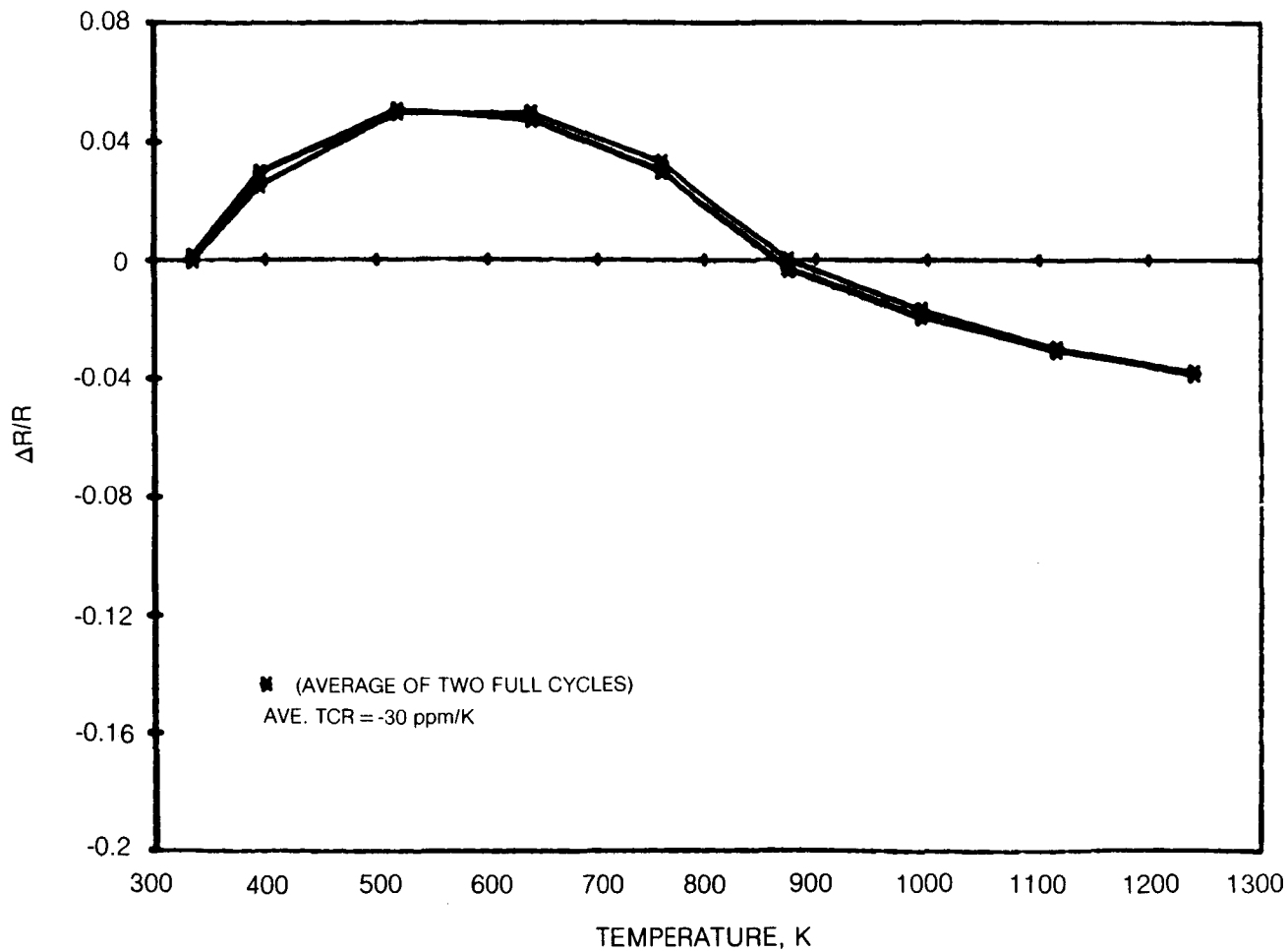
Figure 15. Change in Average Electrical Resistance vs Temperature of FeCrAl Mod #8 at Different Rates of Heating and Cooling at 50K/min
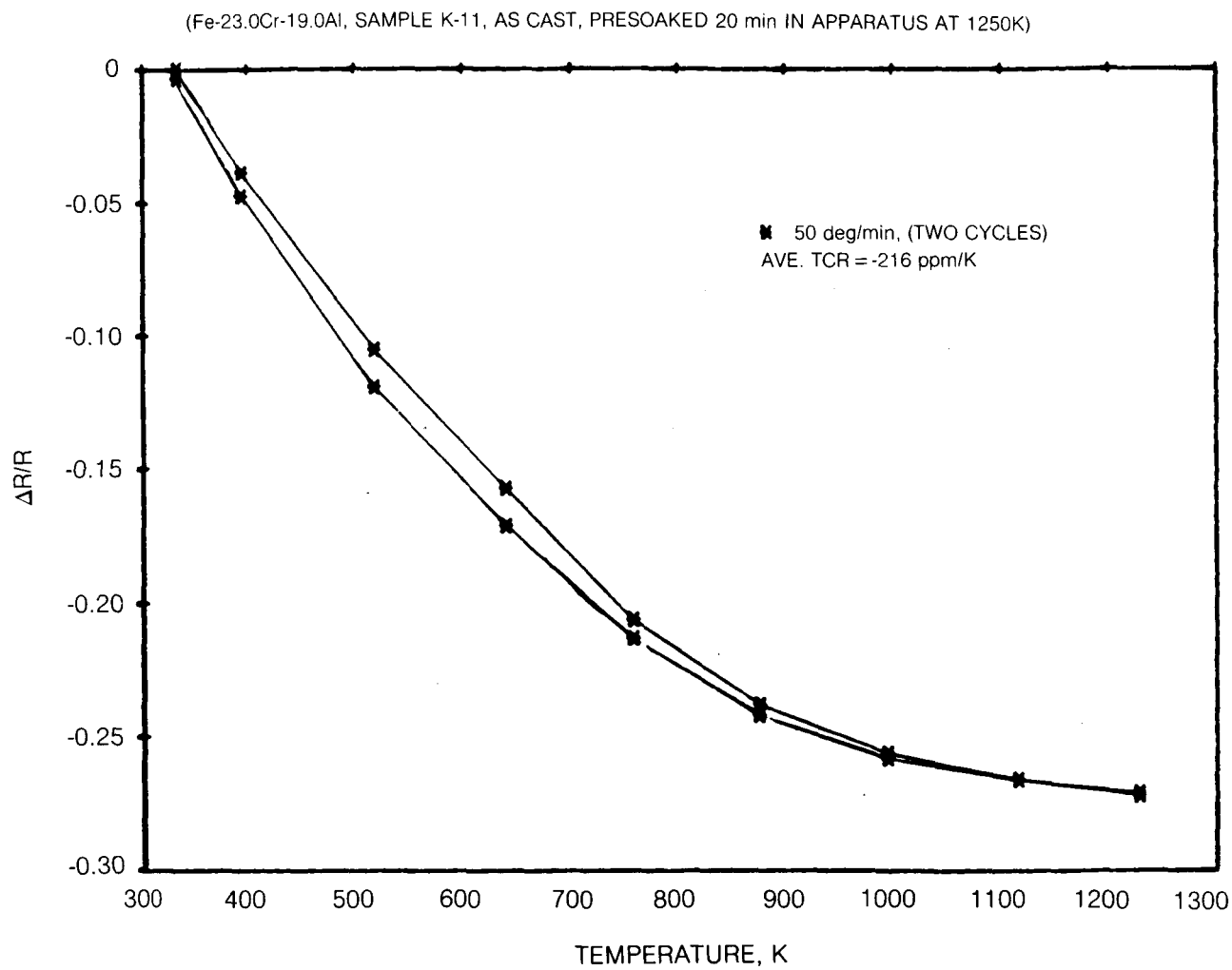
Figure 16. Change in Average Electrical Resistance vs Temperature of FeCrAl Mod #7 at 50 deg/min

(Fe-13.0Cr-24.0Al, SAMPLE K-14, AS CAST, PRESOAKED 20 min IN APPARATUS AT 1250K, WITH NEW COMPUTER SYSTEM, EST. ERROR ± 100 ppm)
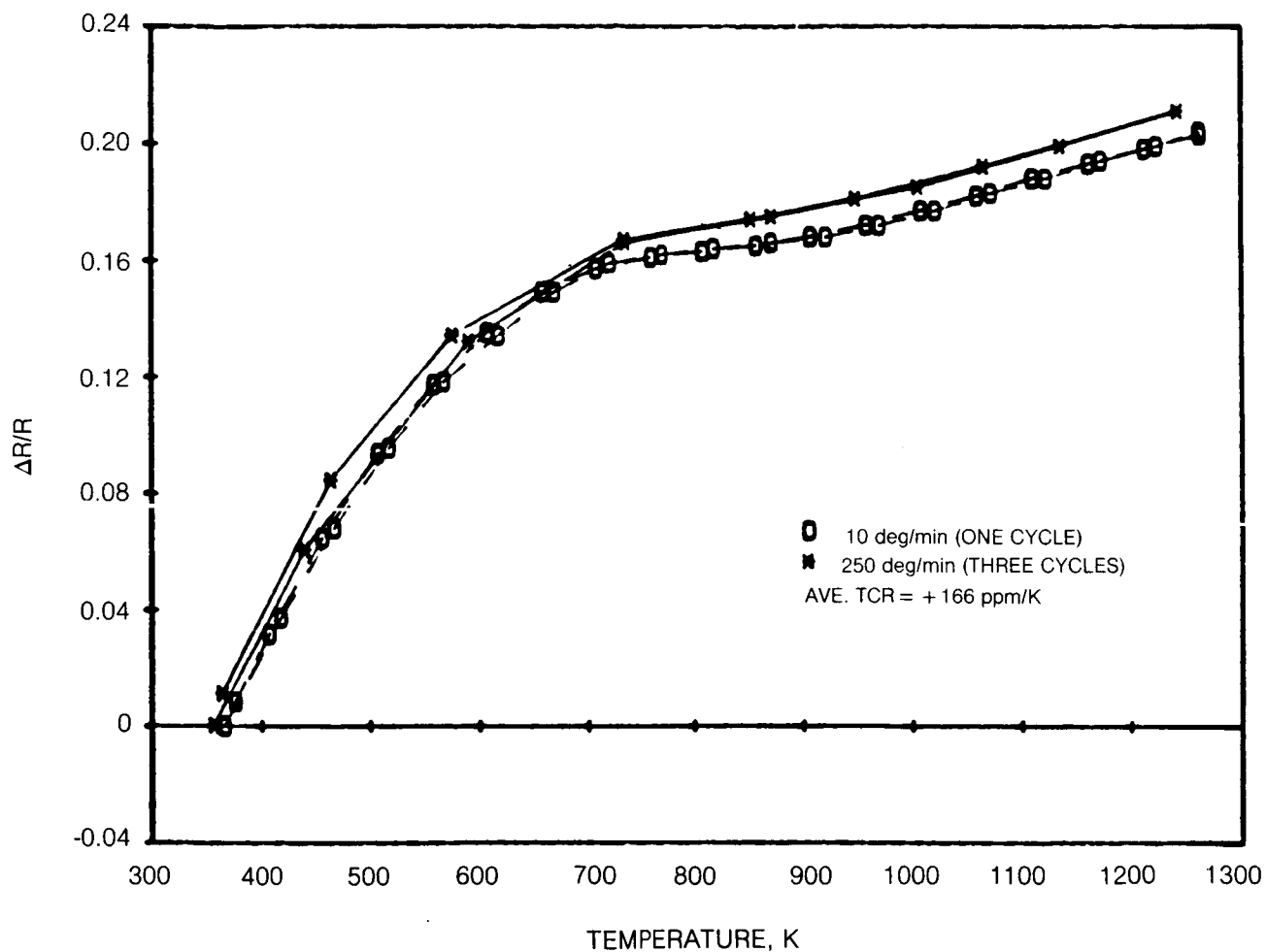
□ 10 deg/min (ONE CYCLE)
✕ 250 deg/min (THREE CYCLES)
AVE. TCR = + 166 ppm/K

Figure 17. Change in Average Electrical Resistance vs Temperature of FeCrAl Mod #10 at Different Rates of Heating and Cooling

(Fe-10.6Cr-11.9Al, SAMPLE K-5, PRETEST HEAT TREATMENT — 3 hrs IN ARGON AT 1473K, IN ALUMINA
TUBE WRAPPED IN Ta FOIL, CARBON HEATER + PRESOAKED 20 min IN APPARATUS AT 1250K,
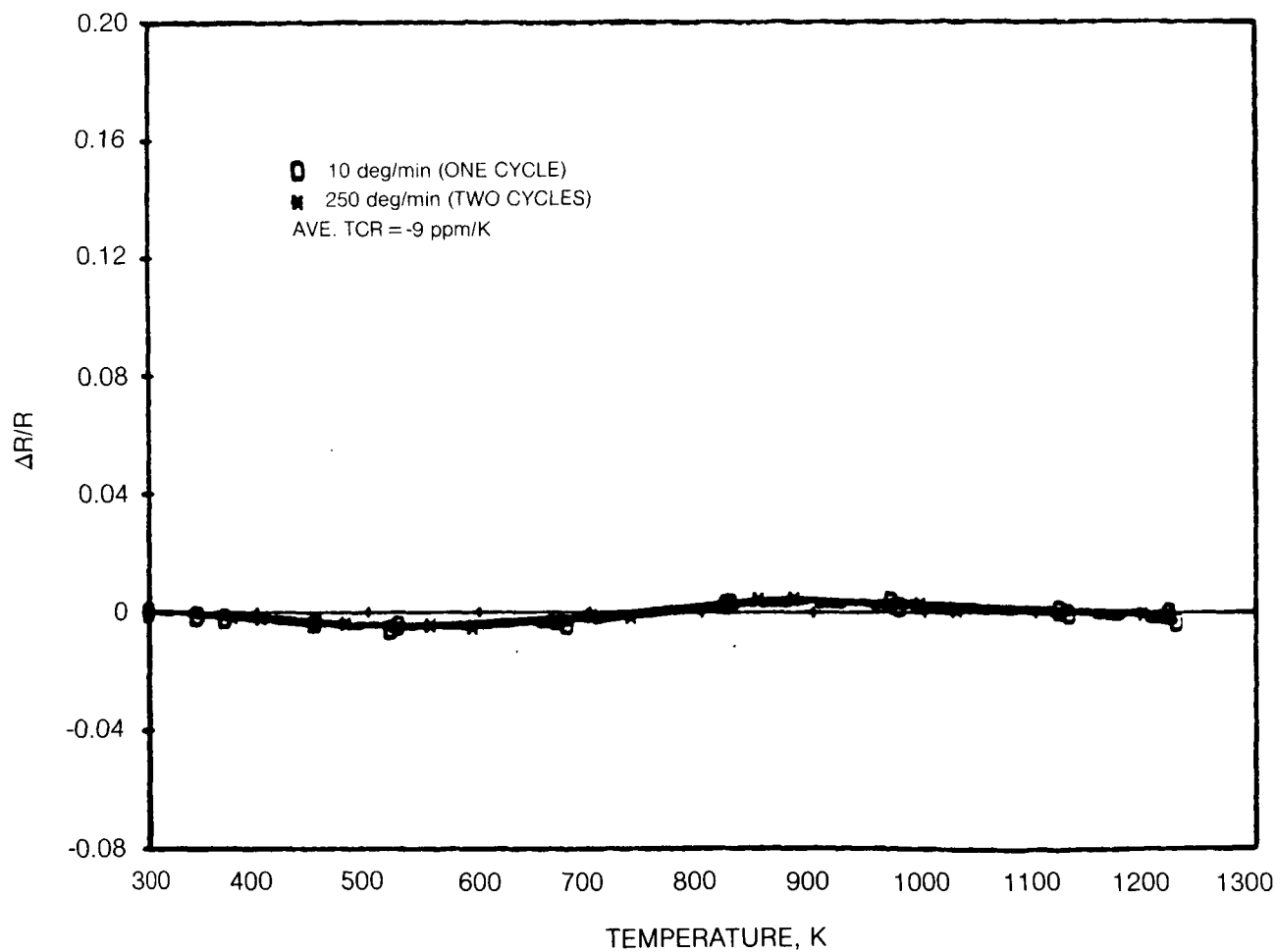WITH NEW COMPUTER AND ULTRA STABLE REFERENCE RESISTOR, EST. ERROR ± 50 ppm)

Figure 18. Change in Average Electrical Resistance vs Temperature of FeCrAl Mod #3 at Different Rates of Heating and Cooling

(Fe-13.8Cr-11.2Al, SAMPLE K-9, PRETEST HEAT TREATMENT-3 hrs IN ARGON AT 1473 K, IN ALUMINA TUBE WRAPPED IN Ta FOIL, CARBON HEATER + PRESOAKED 20 min IN APPARATUS AT 1250K, EST. ERROR ± 50 ppm)
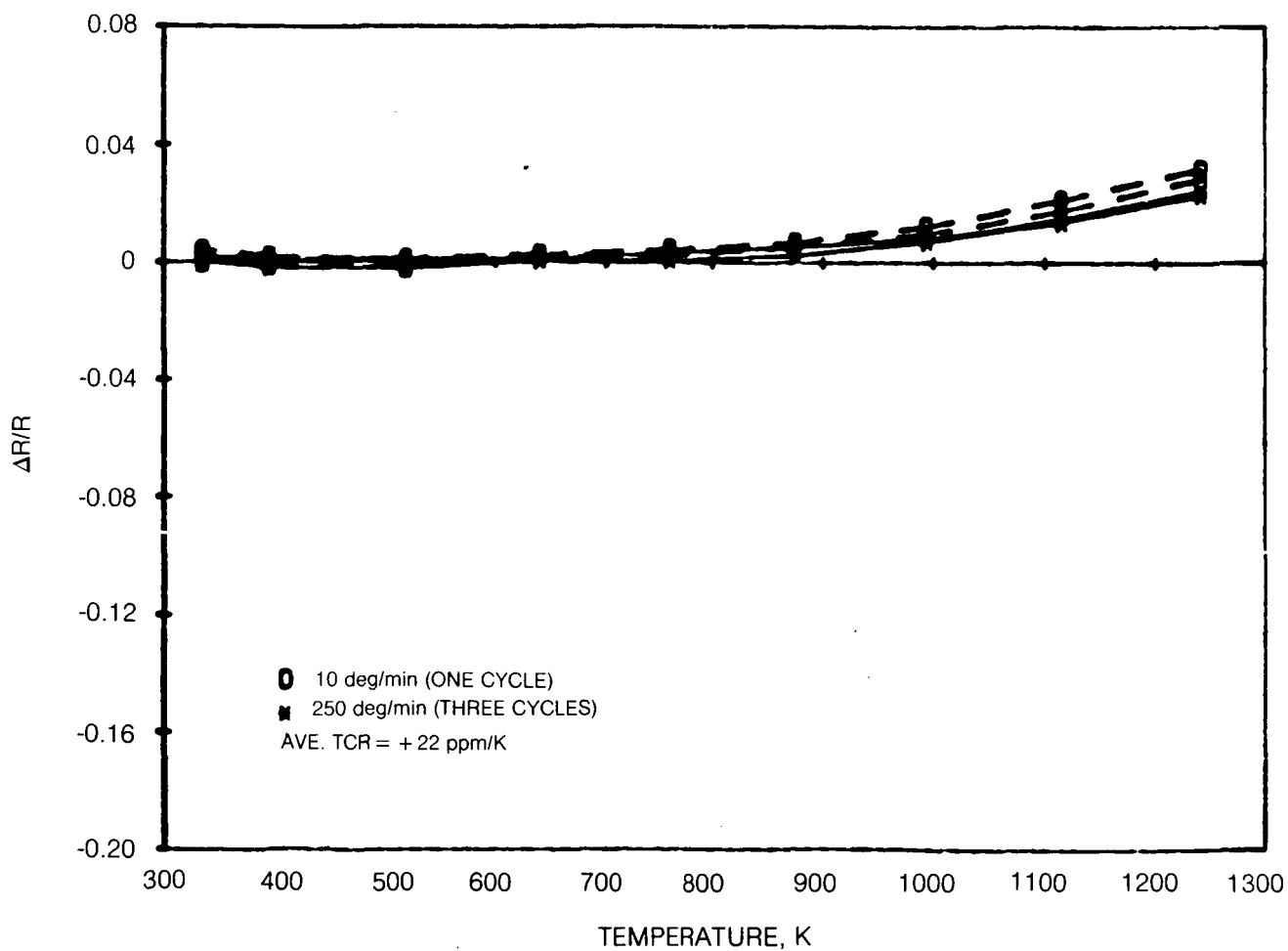
Figure 19. Change in Average Electrical Resistance vs Temperature FeCrAl Mod #5 at Different Rates of Heating and Cooling

(Fe-10.6Cr-11.9Al, SAMPLE K-5, PRETEST HEAT TREATMENT — 3 hrs IN ARGON AT 1473 K,
IN ALUMINA TUBE WRAPPED IN Ta FOIL, CARBON HEATER + PRESOAKED 20 min. IN APPARATUS AT 1250 K,
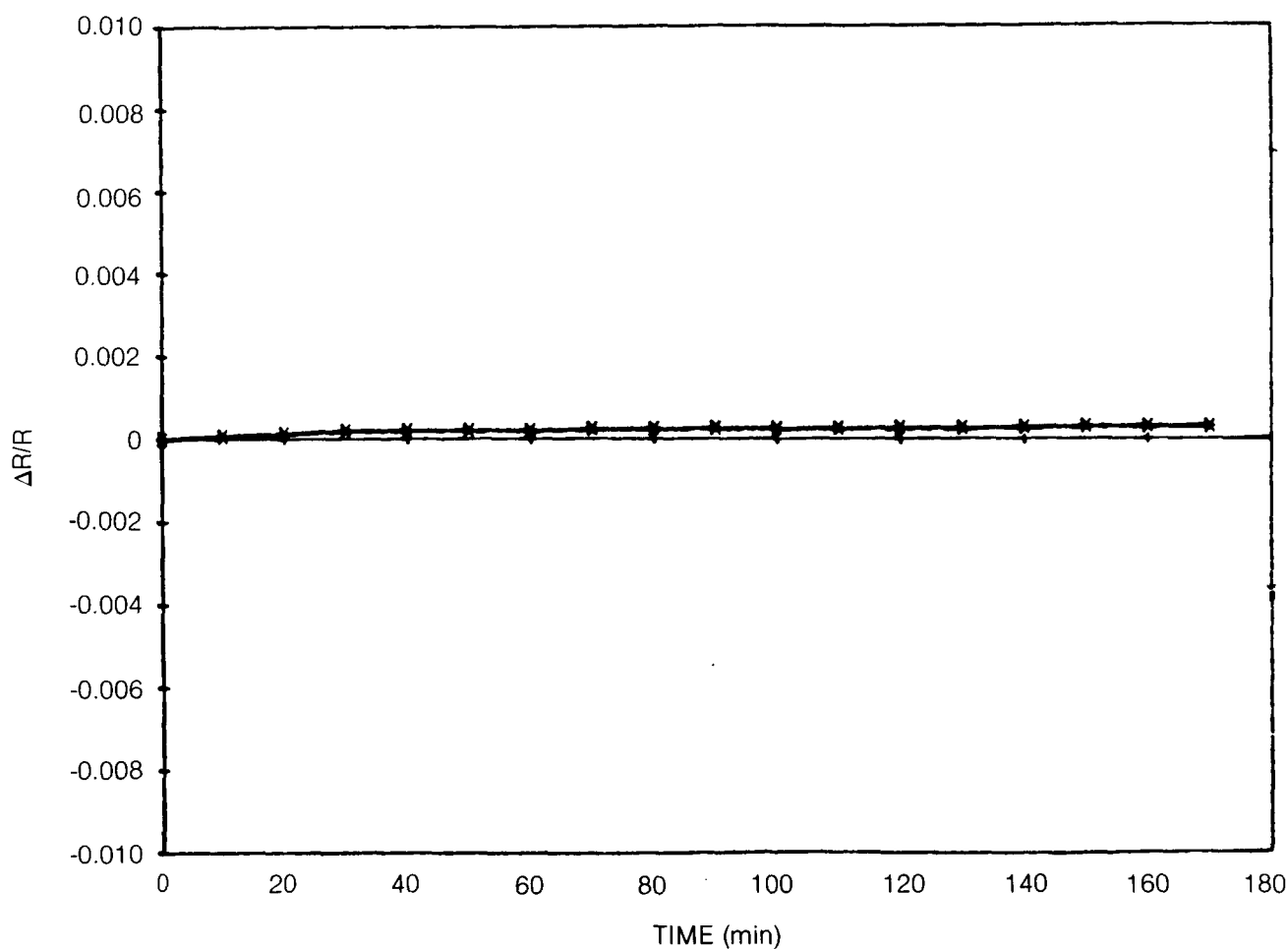EST. ERROR ± 100 ppm)

Figure 20. Electrical Resistance Drift of FeCrAl Mod #3 Over 3 Hour Period at 1250 K in Air

(PRETEST HEAT TREATMENT 1200°C, 3 hrs, ARGON)

○ — KANTHAL A-1, Fe-22Cr-5.7Al-0.5Co
△ — MOD #1, Fe-18Cr-15Al
□ — MOD #2, Fe-17Cr-10.5Al
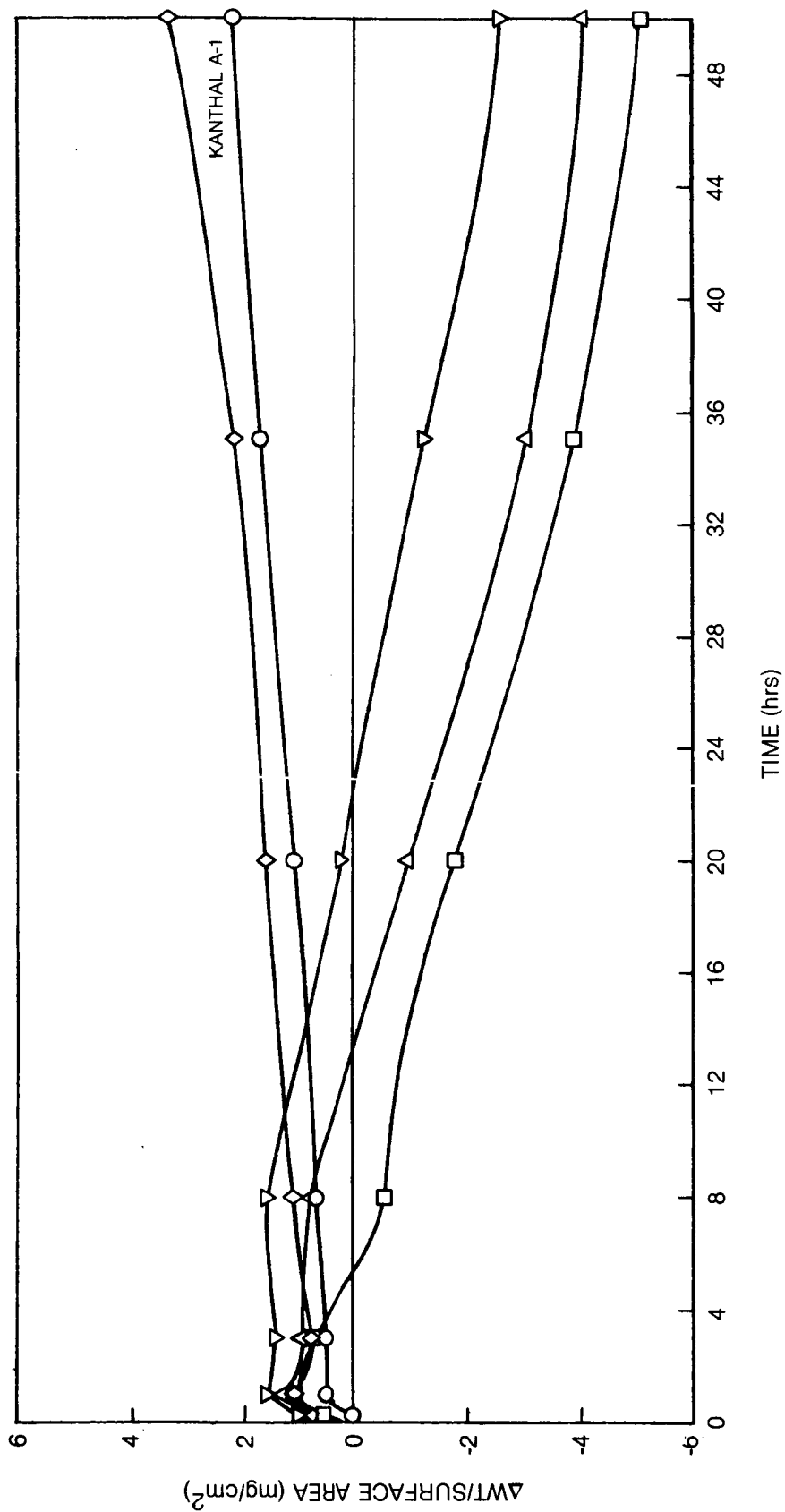◇ — MOD #3, Fe-10.6Cr-11.9Al
▽ — MOD #4, Fe-20Cr-8Al

Figure 21. Weight Change of FeCrAl Alloys Exposed to Air at 1250 K

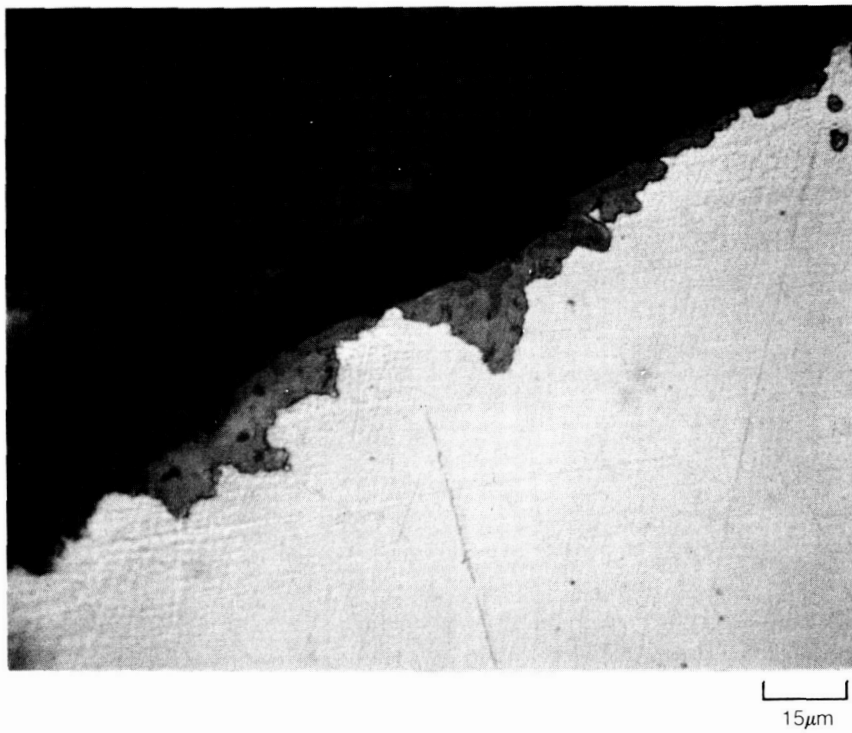AFTER 50 hrs, STATIC AIR, 1250 K

15μm

Figure 22. Transverse Section of Oxidized Surface of FeCrAl Mod #3, Fe-10.6Cr-11.9Al

84—9—35—9
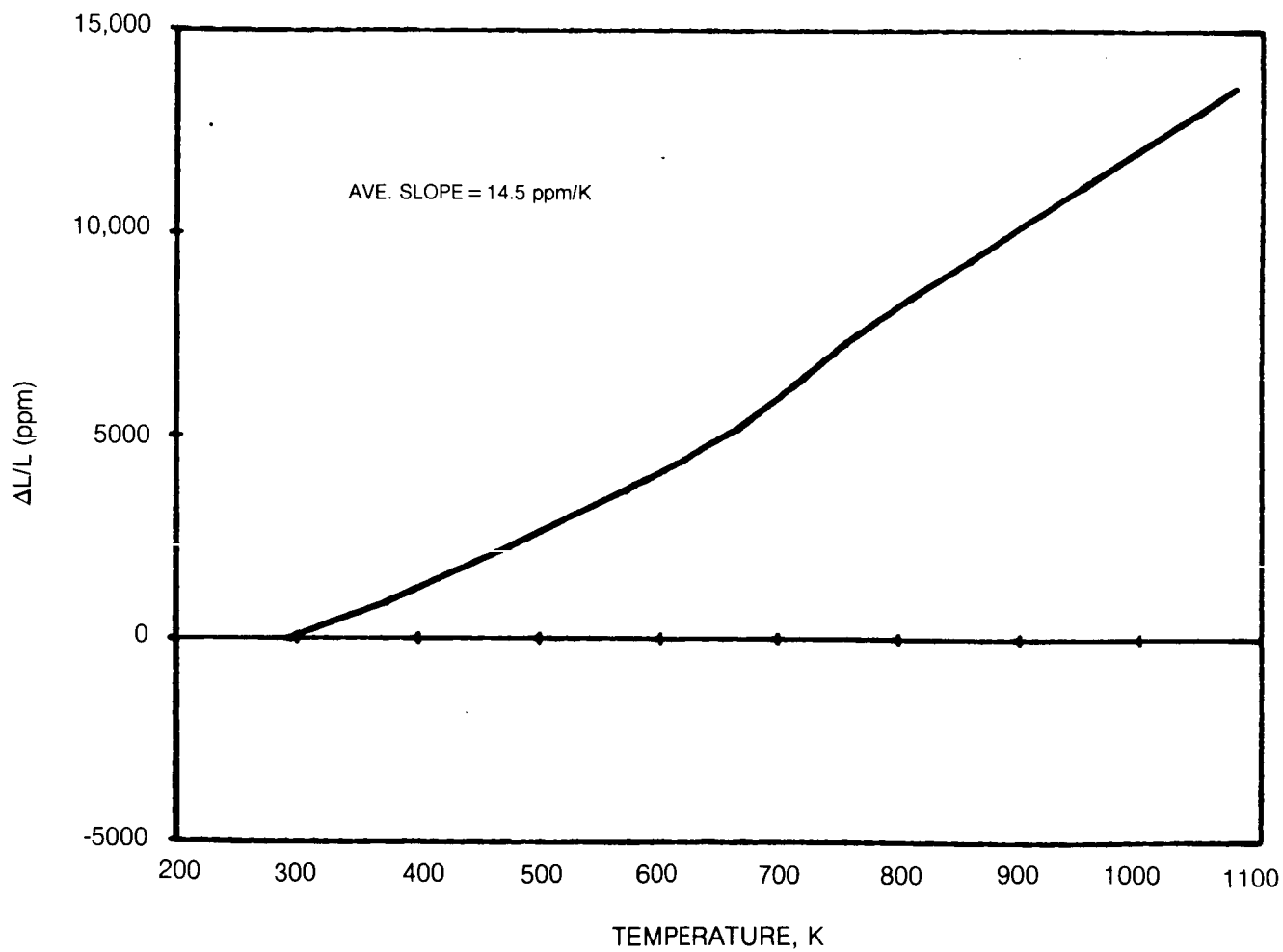
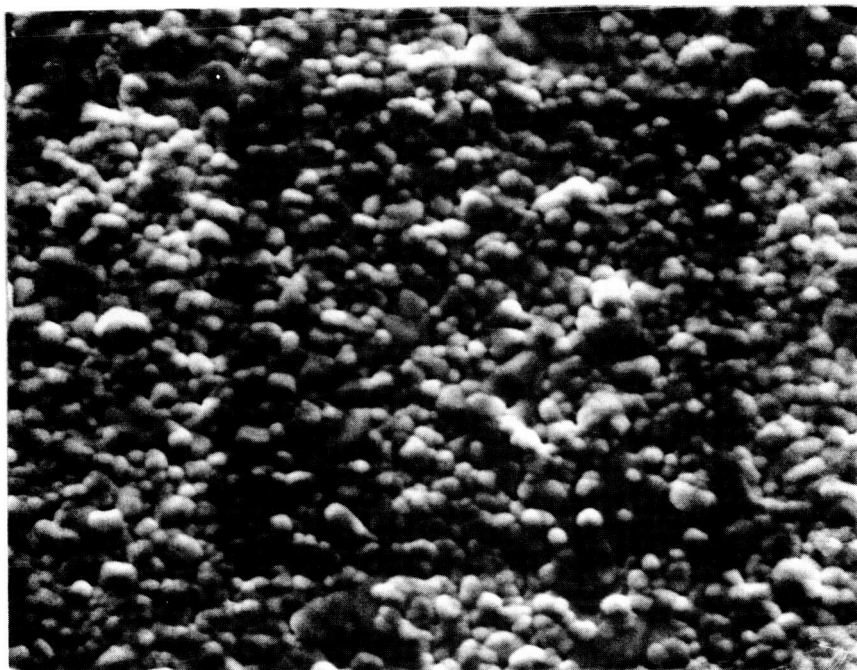**Figure 23. Thermal Expansion of FeCrAl Mod #3, Fe-10.6 Cr-11.9 Al, In Air**
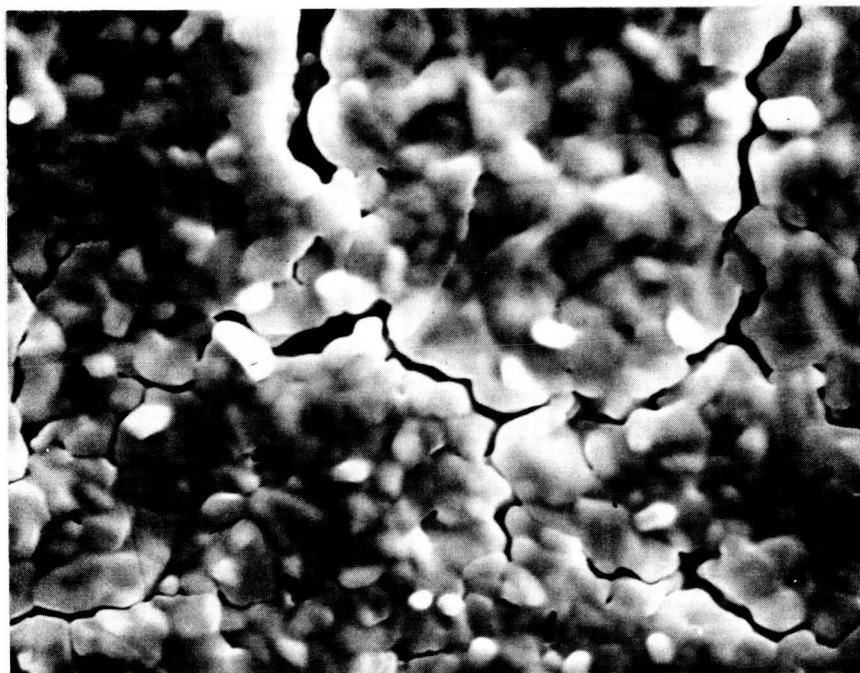
5μm

Figure 24a. As Sputtered Kanthal A-1 Gage

5μm

Figure 24b. Sputtered Kanthal A-1 Gage After 1250°K Exposure, Argon + Air

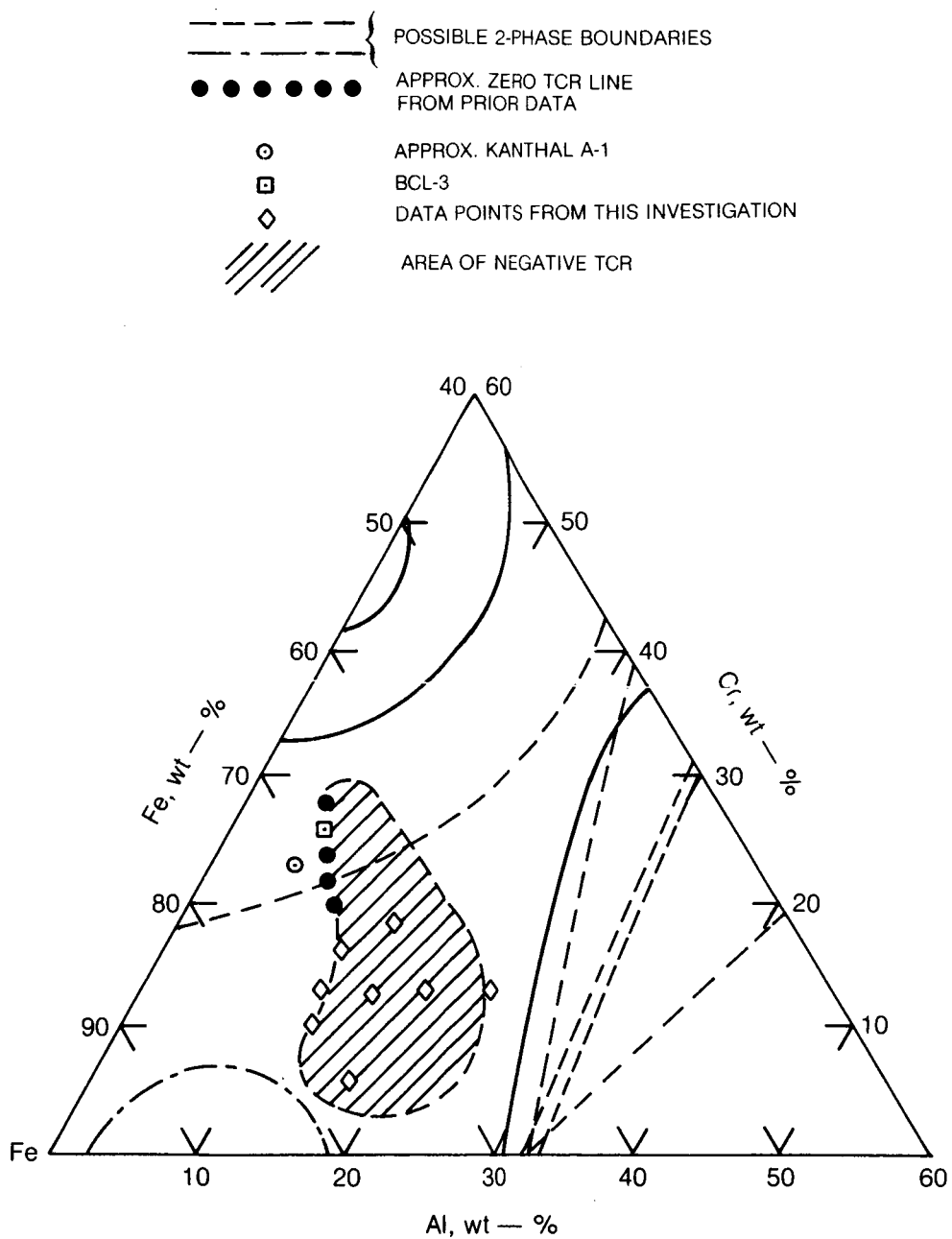**Figure 25. Estimated 873K Isotherm of Fe-Cr-Al System**
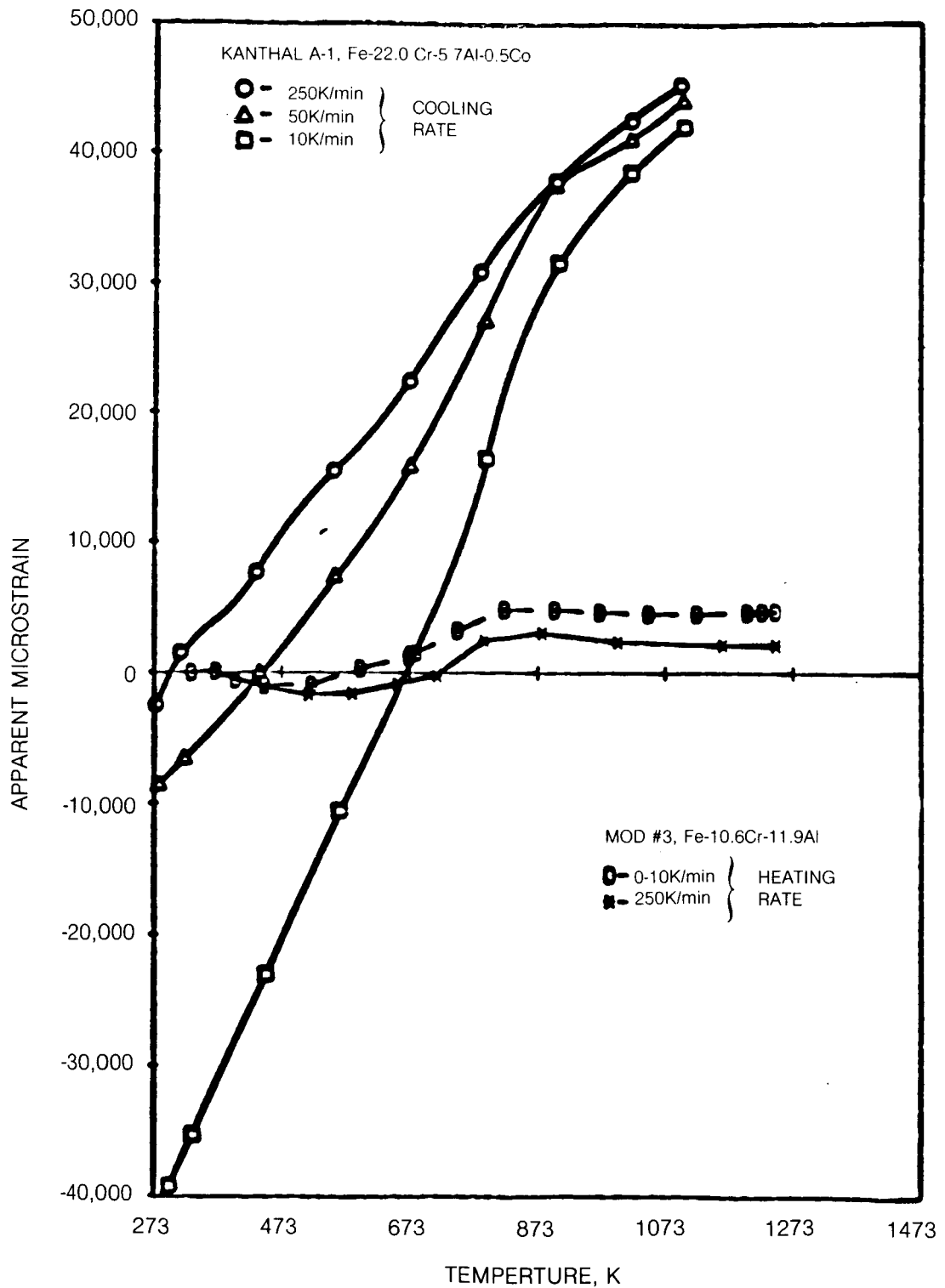
Figure 26. Cooling Curves of Commercial Kanthal A-1 Wires and Heating Curves of Mod #3, both Preannealed 2 Hours at 1153K

APPENDIX I

LITERATURE SOURCES

APPENDIX I

LITERATURE SOURCES

1. McFarland, K. H. and J. Dimeff: Problems Involved in Precision Measurements with Resistance Strain Gages, *Advisory Group for Aeronautical Research and Development*, Report 12, North Atlantic Treaty Organization, February 1956.

2. Andersson, P. and G. Backstrom: Electrical Resistance of Evanohm under Pressure, *Rev. Sci. Instrum.*, Vol. 46, No. 9, September 1975, pp. 1292-1293.

3. Cedergren M. and G. Backstrom: Strain Gauge Measurements of Volume Changes in Polymorphic Transitions under Pressure, *The Review of Scientific Instruments*, Vol. 43, No. 4, April 1972, pp. 686-688.

4. Tomaszewicz, P. and G. R. Wallwork: Iron-Aluminum Alloys: A Review of Their Oxidation Behavior, *Reviews on High Temperature Materials*, Vol. 4, #1 (1978), pp. 75-105.

5. Dils, R. R. and P. S. Follansbee: Superalloy Sensors, *Superalloys: Metallurgy and Manufacture*, Proceedings of the Third International Symposium, September 12-15, 1976, pp. 37-44.

6. Keusseyan, R. L. and Che-Yu Li: Precision Strain Measurement at Elevated Temperatures Using a Capacitance Probe, *Journal of Testing and Evaluation*, JTEVA, Vol. 9, No. 3, May 1981, pp. 214-217.

7. Lowell, C. E., R. G. Garlick, and B. Henry: Thermal Expansion in the Nickel-Chromium-Aluminum and Cobalt-Chromium-Aluminum Systems to 1200°C, National Aeronautics and Space Administration, NASA TM X-3268, August 1975.

8. Kammer, E. W. and I. Vigness: Lattice Defects and Strain-Gage Factors, *Society for Experimental Stress Analysis Proceedings*, Vol. XV, No. 1, May, 1957.

9. Nash, P. and D. R. F. West: Phase Equilibria in the Ni-Ta-Al System, *Metal Science*, December 1979, pp. 670-676.

10. Hamajima, T. and S. Weissmann: Thermal Equilibria and Mechanical Stability of Ti_3 Al Phase in Ti-Mo-Al Alloys, *Metallurgical Transactions A*, Vol. 6A, August 1975, pp. 1535-1539.

11. Rolnick, H.: Tension Coefficient of Resistance of Metals, <u>Physical Review</u>, August 1, 1930, Vol. 36, pp. 506-512.

12. Gysler, A. and S. Weissman: Effect of Order in Ti_3Al Particles and of Temperature on the Deformation Behavior of Age-hardened Ti-Al Alloys, <u>Materials Science and Engineering</u>, 27 (1977) pp. 181-193.

13. Butler, S. R., J. E. Hanlon and R. J. Wasilewski: Electric and Magnetic Properties of B2 Structure Compounds: NiAl, CoAl, <u>J. Phys. Chem. Solids</u>, Pergamon Press 1969, Vol. 30, pp. 1929-1934.

14. Mendiratta, M. G. and H. A. Lipsitt: Steady-State Creep Behaviour of Ti_3Al-Base Intermetallics, <u>Journal of Materials Science 15</u> (1980) pp. 2985-2990.

15. Clark, D., K. S. Jepson, and G. I. Lewis: A Study of the Titanium-Aluminum System up to 40 At.-% Aluminum", <u>Journal of the Institute of Metals</u>, 1962-63, Vol. 91, pp. 197-203.

16. Chandler, R. L. and E. J. Dent: Temperature Compensated Strain Gauges, <u>Electronic Engineering</u>, July 1960, pp. 414-421.

17. Bertodo, R.: Resistance Strain Gauges for the Measurement of Steady Strains at High Temperatures, <u>Proc. Instn. Mech. Engrs.</u> 1963-64, Vol. 178, Pt. 1, No. 34, pp. 907-926.

18. Sastry, S. M. L. and H. A. Lipsitt: Ordering Transformations and Mechanical Properties of Ti_3Al and Ti_3Al-Nb Alloys, <u>Metallurgical Transactions A</u>, Vol. 8A, October 1977, pp. 1543-1552.

19. Schafrik, R. E.: Dynamic Elastic Moduli of the Titanium Aluminides, <u>Metallurgical Transactions A</u>, Volume 8A, June 1977, pp. 1003-1006.

20. Lipsitt, H. A., D. Shechtman, and R. E. Schafrik: The Deformation and Fracture of Ti Al at Elevated Temperatures, <u>Metallurgical Transactions A</u>, Vol. 11A, August 1980, pp. 1369-1375.

21. Easterling, K. E.: High Temperature Resistance Strain Gauges, <u>Brit. J. Appl. Phys.</u>, 1963, Vol. 14, pp. 79-84.

22. Bertodo, R.: Precious Metal Alloys for High-Temperature Resistance Strain Gauges, <u>Brit. J. Appl. Phys.</u> (J. Phys. D), 1968, Ser. 2, Vol. 1, pp. 1743-1752.

LITERATURE SOURCES (Cont'd)

23.   Weymouth, L. J., J. E. Starr and J. Dorsey: Bonded Resistance Strain
      Gages, Manual on Experimental Stress Analysis, Chapter II, Experimental
      Mechanics, pp. 112-120.

24.   Lemcoe, M. M.: Final Report on Development of Strain Gages for Use to 1311
      K (1900 F), Prepared for National Aeronautics and Space Administration,
      July 10, 1974, NASA CR-132485.

25.   Lemcoe, M. M.: Final Report on Characterization of BCL Strain Gages for
      Use to 1366 K (2000 F), Prepared for National Aeronautics and Space Admin-
      istration, August 27, 1975, NASA-CR-132739.

26.   Lemcoe, M. M.: Development of High-Temperature Biaxial-Strain Transducer
      for Use to 1400°F (760°C), Society for Experimental Stress Analysis,
      May 14-19, 1978, SESA Spring Meeting.

27.   Lemcoe, M. M.: The Development of a Low Z Strain Transducer, Defense
      Technical Information Center Technical Report, September 26, 1975.

28.   Bertodo, R.: High Temperature Strain Gauges for Turbo-Jet Components -
      Advantages of Platinum Alloy Resistance Wires, Platinum Metals Review, Vol.
      8, #4, October 1964, pp. 128-130.

29.   Dorsey, J.: Linearization of Transducer Compensation, ISA, 1977, pp. 439-
      442.

30.   Symposium on Elevated Temperature Strain Gages, ASTM Special Technical
      Publication No. 230, 1958.

31.   Lemcoe, M. M.: Characteristics of Two Commercial High-Temperature Electric
      Resistance Strain Gages, Liquid Metal Engineering Center, August 15, 1967.

32.   Bertodo, R.: Resistance Strain Gauges for the Measurement of Steady
      Strains at High Temperatures, Proc. Inst. Mech. Engrs. 1963-1964, Vol. 178,
      Pt. 1, No. 34, pp. 907-926.

33.   Weise, R. A. and Foster, J. H.: High Temperature Strain Gage System for
      Application to Turbine Engine Components, Air Force Wright Aeronautical
      Laboratories, AFWAL-TR-80-2126, Final Report for Period June 1976 - August
      1980.

34.   High Temperature Static Strain Sensor Development Program, OATL81-13, April
      1981, United Technologies Research Center.

LITERATURE SOURCES (Cont'd)

35. Blackburn, M. J.: The Ordering Transformation in Titanium:Aluminum Alloys Containing up to 25 at. pct Aluminum, Transactions of the Metallurgical Society of AIME, Vol. 239, August 1967, pp. 1200-1208.

36. Mendiratta, M. G.: Tensile Properties to 650°C and Deformation Structures in a Precipitation-Strengthened Ti-Al Alloy, Metallurgical Transactions, Vol. 5, May 1974.

37. Blackburn, M. J. and M. P. Smith: The Understanding and Exploitation of Alloys Based on the Compound TiAl (γ Phase), Air Force Materials Laboratory, AFML-TR-78-78, June 1978.

38. Blackburn, M. J. and M. P. Smith: Research To Conduct an Exploratory Experimental and Analytical Investigation of Alloys, Air Force Wright Aeronautical Laboratories, AFWAL-TR-80-4175, November 1980.

39. O'Connell, T. E.: Study of Intermetallic Compounds, Air Force Materials Laboratory, AFML-TR-79-4177, December 1979.

40. Ti/Al Design/Cost Trade-Off Analysis, Air Force Aero-Propulsion Laboratory, AFAPL-TR-78-74, October 1978.

41. Samsonov, G. V., N. G. Kaidash, and P. P. Chastokolenko, Structure and Properties of Titanium-Aluminide Diffusion Coatings on Carbon Steel.

42. Andreyev, O. N., I. I. Kornilov: Investigation of the Effect of Certain Elements on the Heat Resistance of Titanium Aluminide Ti_3Al, Department of the Army, March 19, 1974.

43. Hertz, W. H.: An Investigation of Various Properties of Nickel Aluminide - Part III. Investigation of the Intermetallic Compounds of Aluminum, Wright Air Development Center, Technical Report 52-291, April 1955.

44. Lowell, C. E. and G. J. Santoro: The 1200°C Cyclic Oxidation Behavior of Two Nickel-Aluminum Alloys (Ni_3Al and NiAl) with Additions of Chromium, Silicon, and Titanium, National Aeronautics and Space Administration, NASA TN D-6838, June 1972.

45. Herz, W. H.: An Investigation of Various Properties of NiAl, Wright Air Development Center, WADC Technical Report 52-291, Part 2, August 1954.

46. Zelenkov and E. N. Osokin: Effects of Phase Transitions Upon Some Physical Properties of the Compound Ti_3Al and Its Alloys.

47. Smialek, J. L. and R. F. Hehemann: Transformation Temperatures of Marten-site in Beta-Phase Nickel Aluminide, National Aeronautics and Space Admin-istration, NASA TM X-2654, October 1972.

48. McCoy, H. E., Jr. and D. L. McElroy: Electrical Resistivity Anomaly in Nickel-Base Alloys, Transactions of the ASM, Vol. 61, 1968, pp. 730-741.

49. Yamaguchi, Y., D. A. Kiewit, T. Aoki, and J. O. Brittain: Electrical Resistivity of NiAl, CoAl, NiGa, and CoGa, Journal of Applied Physics, Volume 39, No. 1, January 1968, pp. 231-232.

50. Rtishchev, V. V., Yu. A. Roshchin, and G. V. Vasyukhina: An Investigation of High-Temperature Wire Resistance Strain Gauges of E/617 Alloy.

51. Giggins, C. S., E. J. Felten and F. S. Pettit: The Adhesion of Al_2O_3 Scales on Alloys, Proceedings of the 1974 Triservice Corrosion of Military Equipment Conference, 29-31 October 1974, AFML-TR-75-42, Vol. I, September 1975, pp. 253-268.

52. Savitsky, E. M.: The Influence of Temperature on the Mechanical Properties of Metals and Alloys, Stanford University Press, Stanford, California, 1961.

53. Bertodo, R.: Platinum Metal Alloys for the Measurement of Strains at High Temperature.

54. Skelly, D. W., J. T. Furey, G. J. Sewell, B. C. Wagner, J. H. Foster, C. J. Watters, and W. Cardwell: Thin Film Dynamic Strain Gauges for Jet Engine Compressors.

55. Hanafee, J. E.: Pressure Dependence of the Electrical Resistance of Strain Gauges.

56. Nartova, T. T. and N. I. Shirokova: Phase Equilibrium and Creep Strength of Ti-Zr-Al Alloys.

57. Nartova, T. T. and G. G. Sopochkin: Investigation of the Phase Structure of Ti_3Al-Nb Alloys.

58. Goryachev, Yu. M. and T. G. Kutsenok: Effect of Alloying on the Electro-conductivity of Cerium Sulfide, Translated from Poroshkovaya Metallurgiya, No. 1(49), pp. 95-98, January, 1967.

59. Kornilov, I. I., V. S. Mikheyev and K. M. Konstantinov: Study of the Volume Resistivity of Alloys of the System Ti-Al at Temperatures Ranging from Room to 1200°C.

60. Nartova, T. T., M. A. Volkova, E. V. Meleshko, and Yu. N. Stepanov: Influence of Zirconium, Molybdenum and Tungsten on the Structure and Properties of the Compound Ti_3Al.

61. Kammer, E. W. and T. E. Pardue: Electric Resistance Changes of Fine Wires During Elastic and Plastic Strains.

62. Loasby, R. G.: The γ Phase in Uranium Alloys.

63. Drew, D. A.: Developments in Methods of Measuring Stresses in Compressor and Turbine Blades on Test Bed and In Flight.

64. Milek, J. T.: Aluminum Oxide Data Sheets: U. S. Department of Commerce, National Bureau of Standards, Institute for Applied Technology, March 1964.

65. Bowen, H. K.: Ceramics as Electrical Materials, Massachusetts Institute of Technology, Industrial Liaison Program, Vol. 5.

66. Meiksin, Z. H. and W. D. Humbel: Thick-Film Strain Gauges and Pressure Transducers, Electronics Letters, 27th March 1980, Vol. 16, No. 7.

67. Lemcoe, M. M.: Development of High-temperature Biaxial-strain Transducer for Use to 1033°K (1400°F), Experimental Mechanics, February 1979, pp. 56-62.

68. Lemcoe, M. M.: Development of Electric Resistance Strain Gage System for Use to 2000 F, ISA, 1975.

69. Lemcoe, M. M.: Accuracy of Strain Measurements at Elevated Temperatures with Electric Resistance Strain Gages, Advanced Testing Techniques, ASTM STP 476, American Society for Testing and Materials, 1970, pp. 12-34.

70. Lemcoe, M. M. et al.: Attaching of Strain Gages to Substrates, United States Patent, 4,195,279, March 25, 1980.

71. Selman, G. L.: The Platinum-Molybdenum System - The Formation of Intermediate Phases.

72. High Temperature Strain Gauges - Advantages of Platinum Metal Alloys, _Platinum Metals Review_, Vol. 12, #3, 1968.

73. Darling, A. S., G. L. Selman, and A. A. Bourne: Dispersion Strengthened Platinum - Improved High Temperature Creep Properties, _Platinum Metals Review_, Vol. 12, #1, 1968, pp. 7-13.

74. Coles, B. R.: Electronic Structure and Properties of Palladium and its Alloys, _Platinum Metals Review_, Vol. 11, #3, 1967.

75. Tungsten-Platinum Alloy Strain Gauges, _Platinum Metals Review_, Vol. 11, #2, 1967.

76. Selman, G. L. and A. A. Bourne: Dispersion-Strengthened Rhodium-Platinum - A New Material for High-Temperature Structural Applications, _Platinum Metals Review_, Vol. 20, #3, 1976, pp. 86-90.

77. Rhodium and Iridium of Improved Ductility, _Platinum Metals Review_, Vol. 17, #3, 1973.

78. Selman, G. L., P. J. Ellison, and A. S. Darling: Carbon in Platinum and Palladium - Solubility Determinations and Diffusion at High Temperatures, Platinum Metals Review, Vol. 14, #1, 1970, pp. 14-20.

79. Skinner, D. and A. P. Miodownik: Order-Disorder Transformations in some Iron-Nickel-Platinum Alloys, _Platinum Metals Review_, Vol. 20, #1, 1978, pp. 21-24.

80. Holcombe, C. E., Jr.: Intermetallic Compounds of Yttrium and Hafnium with Platinum, _Journal of Less-Common Metals_, 44 (1976) pp. 331-335.

81. Darling, A. S.: Electron Configuration and Crystal Structure of Platinum Metal Alloys, _Platinum Metals Review_, Vol. 11, #4, 1967, pp. 138-140.

82. Darling, A. S.: Electron Concentration as a Guide to Alloying Behaviour - Engel-Brewer and the Platinum Metals, _Platinum Metals Review_, Vol. 13, #2, 1969, pp. 53-56.

83. Darling, A. S., G. L. Selman and R. Rushforth: Platinum and the Refractory Oxides - I-Compatibility and Decomposition Processes at High Temperatures, _Platinum Metals Review_, Vol. 14, #2, 1970. pp. 54-60.

84. Strength and Ductility of Iridium, _Platinum Metals Review_, Vol. 14, #2, 1970.

LITERATURE SOURCES (Cont'd)

85. Darling, A. S., G. L. Selman and R. Rushforth: Platinum and the Refractory
     Oxides - II-Influence of Geometry on the Reacting Systems, _Platinum Metals
     Review_, Vol. 14, #3, 1970, pp. 95-102.

86. Darling, A. S., G. L. Selman and R. Rushforth: Platinum and the Refractory
     Oxides - III-Constitutional Relationships in the Alloys Formed, _Platinum
     Metals Review_, Vol. 14, #4, 1970, pp. 124-130.

87. Darling, A. S., G. L. Selman, and R. Rushforth: Platinum and the
     Refractory Oxides - IV-The Performance in Service of Platinum
     Thermocouples, _Platinum Metals Review_, Vol. 15, #1, 1971, pp. 13-18.

88. Ott, D. and C. J. Raub: The Affinity of the Platinum Metals for Refractory
     Oxides - Reactions Under Reducing Conditions, _Platinum Metals Review_, Vol.
     20, #3, 1976, pp. 79-85.

89. High Temperature Thermodynamic Properties of Platinum-Titanium Alloys,
     Platinum Metals Review, Vol. 20, #3, 1976.

90. Potential Uses of Ruthenium-Molybdenum and Ruthenium-Tungsten Alloys,
     Platinum Metals Review, Vol. 20, #4, 1976.

91. Platinum Deposition on Sapphire and Alumina - Sputtered Substrates for
     Ferroelectric Films in Computer Memories, _Platinum Metals Review_, Vol. 18.
     #1. 1974.

92. Selman, G. L., J. G. Day and A. A. Bourne: Dispersion Strengthened
     Platinum - Properties and Characteristics of a New High Temperature
     Material, _Platinum Metals Review_, Vol. 18, #2, 1974, pp. 46-56.

93. Irani, R. S.: Ordering in Platinum Group Metal Alloys, _Platinum Metals
     Review_, Vol. 17, #1, 1973, pp. 21-25.

94. Deposition of Platinum Films by Radio-Frequency Sputtering, _Platinum Metals
     Review_, Vol. 19, #2, 1975.

95. Chaston, J. C.: The Oxidation of the Platinum Metals - A Descriptive
     Survey of the Reactions Involved, Platinum Metals Review, Vol. 19, #4,
     1975, pp. 135-140.

96. McGill, I. R.: Intermetallic Compounds of the Platinum Group Metals -
     Selected Materials and Their Properties, _Platinum Metals Review_, pp. 85-
     89.

97. Jehn, H., R. Volker and M. I. Ismail: Iridium Losses During Oxidation - Reactions at High Temperatures in Low-Pressure Oxygen Atmospheres, Platinum Metals Review, Vol. 22, #3, 1978, pp. 92-97.

98. Burch, R.: The Oxidation State of Rhenium and Its Role in Platinum-Rhenium Reforming Catalysts, Platinum Metals Review, Vol. 22, #2, 1978, pp. 57-60.

99. Platinum Monoxide, Platinum Metals Review, Vol. 22, #2, 1978.

100. Jenkins, J. and M. Lemcoe: Problems Associated with Attaching Strain Gages to Titanium Alloy Ti-6Al-4V, NASA TM X-56044, February 1977.

101. Lemcoe, M.: Final Report - Development of High Temperature Strain Gages, NAS1-11277, NASA-CR-112241, January 1973.

102. Lemcoe, M. M.: Characteristics of LMEC Electrical Resistance Strain Gages Using Armour D Alloy, Contract AT(04-3)-700, June 1970.

103. Easterling, K. E.: High Temperature Resistance Strain Gauges, Brit. J. Appl. Phys., Vol. 14, pp. 79-84.

104. Wu, Tsen-Tai, Liang-cheng Ma and Lin-bao Zhao: Development of Temperature-compensated Resistance Strain Gages for Use to 700°C.

105. Wu, Tsen-Tai, Liang-chen Ma, and Lin-bao Zhao: Development of Self-Temperature-Compensated Resistance Strain Gauges for Use to 973K(1292°F), SESA.

106. Rivlin, V. G. and G. V. Raynor: Phase Equilibria in Irony Ternary Alloys - 3: Critical Evaluation of Constitution of Aluminum-Chromium-Iron System, Society for Experimental Stress Analysis, SESA, 1980.

107. Buckman, R. W., Jr.: Consolidation and Fabrication of Vanadium and Vanadium-Base Alloys, Society for Experimental Stress Analysis, SESA, 1980.

108. Zhi-qi, Z. and H. Pei-qing: Development of the Self-Temperature Compensated Resistance Strain Gage Used up to 700 C, The American Society of Mechanical Engineers.

109. Graft, W. H.: Development of High-Temperature Strain Gage Wire.

110. Buschow, K. H. J. and H. J. van Daal: Comparison of Anomalies Observed in U-nad Ce-Intermetallics.

111. Croft, M. and A. Jayaraman: A Comparison of CeS and CeAl$_2$, Solid State Communications, Vol. 35, pp. 203-206.

112. Schobinger-Papamantellos, P., P. Fischer, A. Niggli, E. Kaldis and V. Hildebrandt: Magnetic Ordering of Rare Earth Monochalcogenides: I. Neutron Diffraction Investigation of CeS, NdS, NdSe, NdTe and TbSe, J. Phys. C: Solid State Phys., Vol. 7, 1974.

113. Bartholin, H., A. Waintal, G. Parisot, F. Kervella, and J. P. Senateur: Effect of Pressure on the Crystal Lattice Parameters of CeAl$_2$, PrAl$_2$, YbAl$_2$, and CeS, phys. stat. sol. (a) 61, K87 (1980).

114. Goryachev, Yu. M. and T. G. Kutsenok: Effect of Alloying on the Electroconductivity of Cerium Sulfide.

115. Golikova, O. A.: Conduction in Semiconductors with Lattice Imperfections, Sov. Phys. Semicond., Vol. 10, No. 7, July 1976.

116. Golikova, O. A. and I. M. Rudnik: Mechanism of Conduction in Cerium Sulfide, Sov. Phys. Semicond., Vol. 8, No. 9, March 1975.

117. Bertodo, R.: High-Temperature High-Elongation Resistance Strain Gauges, Journal of Strain Analysis, Vol. 4, No. 3, 1969.

118. Bertodo, R.: Precious Metal Alloys for High-Temperature Resistance Strain Gauges, Brit. J. Appl. Phys. (J. Phys. D), 1968, Ser. 2, Vol. 1.

119. Burley, N. A., R. M. Hess, C. F. Howie: Nicrosil and Nisil: new nickel-based thermocouple alloys of ultra-high thermoelectric stability, High Temperatures - High Pressures, 1980, volume 12, pages 403-410.

120. Burley, N. A., R. L. Powell, G. W. Burns, and M. G. Scroger: The Nicrosil versus Nisil Thermocouple: Properties and Thermoelectric Reference Data, NBS MN-161, April 1978.

121. Mooij, J. H.: Electrical Conduction in Concentrated Disordered Transition Metal Alloys, phys. stat. sol. (a) 17, 521 (1973), pp. 521-530.

122. Mooif, J. H. and M. de Jong: Structural and Electrical Properties of Sputterd CrNi Films, The Journal of Vacuum Science and Technology, Vol. 9, No. 4, pp. 446-449.

123. Day, E. E.: Recent Laboratory Evaluation of High-Temperature Strain Gages to 900 F.

LITERATURE SOURCES (Cont'd)

124. Bean, W. T., Jr.: Progress on Metalfilm Strain Gages.

125. Kemp, R. H.: Advances in Static and Dynamic High Temperature Strain Gage
     Research.

126. Gray, E. I., A. Grossman, and M. R. Rubin: Temperature Compensation of
     High-Temperature Strain Gages.

127. Forlifer, W. R.: Laboratory Evaluation of Nichrome-Foil Strain Gage
     Installations up to 1200 F.

128. Bloss, R. L.: A Facility for the Evaluation of Resistance Strain Gages at
     Elevated Temperatures.

129. Pitts, J. W., E. Buzzard, and D. G. Moore: Resistance Measurement of
     Ceramic-Type Strain Gage Cements.

130. Graft, W. H.: Development of High-Temperature Strain Gage Wire.

131. Shrager, J. J.: Evaluation of Several Gage Configurations Fabricated with
     Armour Alloy 'D'.

132. Moore, D. G.: Bonding Agents for High-Temperature Strain Gages.

133. Hines, F. F.: Foil Gages for High-Temperature Applications.

134. Friedman, R.: Temperature Compensation Techniques.

135. Stewart, R. J.: Elevated Temperature Strain-Gage Investigations at Grumman
     Aircraft Engineering Corporation.

136. Martina, C. K.: High Temperature Strain Gage Evaluator.

137. Yanowitz, H., I. Berman, and A. Bleiweis: Investigation of Strain Gages
     for Long-Time Static Testing to 650 F.

138. Drew, D. A.: High-Temperature Strain Gage Testing at Rolls-Royce.

139. Anderson, B. R.: Development and Application of High-Temperature Strain
     Gages for Stress Measurements in Jet Engines.

140. Brewer, G. A.: The Synthetic Mico Gage.

141. Weast, R. C. and S. M. Selby: Handbook of Chemistry and Physics, Chemical Rubber Company, 1966.

142. The Kanthal Handbook, the Kanthal Corp., 1964.

143. Colin, J. S.: Metals Reference Handbook, Plenum Press, 1967.

144. Grant, H. P., J. S. Przybyszewski and R. G. Claing: Turbine Blade Temperature Measurements using Thin Film Temperature Sensors, NASA CR-165201, 1981.

145. Erickson, J. S., C. P. Sullivan and F. L. VerSnyder: Modern Processing Methods and Investment Casting of the Superalloy Family.

146. Hansen, M.: Constitution of Binary Alloys, McGraw-Hill, 1958.

147. Elliott, R. P.: Constitution of Binary Alloys, First Supplement, McGraw-Hill, 1965.

148. Shunk, F. A.: Constitution of Binary Alloys, Second Supplement, McGraw-Hill. 1969.

149. Fuschillo, N. and R. A. Lindberg: Electrical Conductors at Elevated Temperatures, Tech. Report ASD-TDR-62-481, 1962.

150. Kanthal A-1, Engineering Alloys Digest, Inc., Montclair, N.J., 1970.

151. Evans, R. C.: An Introduction to Crystal Chemistry, Cambridge Univ. Press, 1948.

152. Moffatt, W. G.: Binary Phase Diagrams Handbook, General Electric Company, 1976.

153. Lyman, T.: Metals Handbook, American Society for Metals, 1948.

154. Mullaly, J.: Developmental Coatings by the Sputter Deposition Method, G.P.D. Proposal FP81-146, (1981).

155. Mullaly, J. and P. Allard: Development of Sputtered Techniques for Thrust Chambers, NASA CR-159637, (1979).

156. Bertodo, R.: Platinum Metal Alloys for the Measurement of Strain at High Temperature, Engelhard Industries Tech. Bulletin, V.9, No. 2, 1968.

157. Mr. Giler, Telephone Conversations, Vice President, Kanthal Corp., Bethel, CT.

158. Smeggil, J., Private Communications, United Technologies Research Center.

159. Prof. H. Nowotny, University of Connecticut, Storrs, CT.

160. Platinum, The International Nickel Company, 1968.

161. Palladium, The International Nickel Company.

Instrumentation and Control Technology Office

NASA Lewis Research Center
Attn: Herbert Will
Mail Stop 77/1
Cleveland, OH 44135
(50 copies)

NASA Lewis Research Center
Attn: Gerald A. Boulanger
21000 Brookpark Road
Cleveland, OH 44135
Mail Stop 500/305

NASA Scientific and Technical
  Information Facility
Attn: Acquisitions Branch
P. O. Box 8757
B.W.I. Airport, Md 21240
(22 Copies)

NASA Lewis Research Center
Attn: Library, M. S. 60/3
21000 Brookpark Road
Cleveland, OH 44135
(2 copies)

NASA Lewis Research Center
Attn: Report Control Office,
Mail Stop 60/1
21000 Brookpark Road
Cleveland, OH 44315

General Electric Company
Aircraft Engine Group
Evendale, OH 45215
Attn: Wayne Shaffernocker, MSH-78
      Ronald Weise, MSH-78
      William Stowell

Stanford University
Attn: Dr. R. J. Moffatt
Asst. Prof., Mech. Engr.
Dir. Thermoscience Measurement
  Center
Stanford, CA 94305

Hitec Corporation
Attn: Steve Wnuk
Nardone Industrial Park
Westford, MA 01886

Air Force Wright Aeronautical
  Laboratory
Attn: R. Cox/POTC
Wright Patterson AFB, OH 45433

Air Force Wright Aeronautical
  Laboratory
Attn: Everett E. Bailey/AFWAL/NASA
Wright Patterson AFB, OH 45433

Air Force Wright Aeronautical
  Laboratory
Attn: William Stange/POTC

Air Force Wright Aeronautical Laboratory
Attn: M. Roquemore/POSF
Wright Patterson AFB, OH 45433

UTRC/OATL
Attn: John T. Carroll
Bldg. 30, MS R-23
Palm Beach Gardens Facility
West Palm Beach, FL 33402

Lewis Engineering Company
Attn: C. B. Stegner
238 Wate Street
Naugatuck, CT 06770

Arnold Engineering Development Center
Attn: Marshall Kingery
Arnold Air Force Station, TN 37389

FluiDyne Engr. Corporation
Attn: T. Matsuura
5900 Olson Memorial Highway
Minneapolis, MN 55422

General Electric Company
Attn: George Leperch, A129dD
Aircraft Engine Group
1000 Western Avenue
Lynn, MA 01910

General Electric Company
Attn: Ronald J. Casagrande
Aircraft Equipment Division
50 Fordham Road
Wilmington, MA 01887

Allison Gas Turbine Operations
Attn: John Custer, W-16
General MOtors Corporation
P. O. Box 894
Indianapolis, IN 46206

Allison Gas Turbine Operations
Attn: Ken Cross
P. O. Box 894
Indianapolis, IN 46206

Allison Gas Turbine Opertions
Attn: David Willis
General Motors Corporation
P. O. Box 894
Indianapolis, IN 46206

Allison Gas Turbine Operations
Attn: Ralph Fox
General Motors Corporation
P. O. Box 894
Indianapolis, IN 46206

Battelle Columbus Laboratories
Attn: Ross G. Luce
Energy & Thermal Tech. Section
Columbus, OH 43201

Teledyne CAE
1350 Laskey Road
Toledo, OH 43612
Attn: R. Hugh Gaylord
      Joseph Pacholec

AVCO Corporation
Attn: E. Twarog, Manager
Electronics and Instr.
Lycoming Division
550 South Main Street
Stratford, CT 06497

Thermonetics Corporation
Attn: H. J. Poppendiek
1028 Garnet Avenue
San Diego, CA 92109

Battelle Columbus Laboratories
Attn: M. M. Lemcoe
505 King Avenue
Columbus, OH 43201

Peter K. Stein
4602 East Monterosa
Phoenix, AZ 85018

Pratt & Whitney Aircraft
Main Plant
P. O. Box 2691
West Palm Beach, FL 33402
Attn: John Prosser (MS C-04)
      William Watkins

National Bureau of Standards
Attn: Ken Kreider
Washington, DC 20234

National Bureau of Standards
Attn: George Burns
Inst. for Basic Research
Washington, DC 20234

General Electric Company
Attn: Dr. David Skelley
Bldg. K-1, Room 3B24
P. O. Box 8
Schnectady, NY 12301

Mechanical Technology, Inc.
Attn: R. Hohenberg
968 Albany-Shaker Road
Latham, NY 12110

Garrett Turbine Engine Company
Attn: N. Fred Pratt
P. O. Box 5217
Phoenix, AZ 85010

Boeing Aerospace Company
Attn: Darrell R. Harting
Engineering Laboratories
Seattle, WA 98124

Engelhard
Attn: Ronald G. Braun
Engelhard Industries Div.
228 East 10th Street
Newport, KY 41075

Williams International
2280 West Maple Road
Walled Lake, MI 48088
Attn: Henry Moore, Head,
      Instr. Dept.
      J. H. Johnston

Virginia Polytechnic Institute
  and State University
Attn: W. F. O'Brien, Jr.
Mechanical Engineering Dept.
Blacksburg, VA 24061

Naval Post Graduate School
Attn: Prof. R. P. Shreeve
Department of Aeronutics (Code 67)
Monterey, CA 93940

Pennsylvania State University
Attn: Prof. B. Lakshminarayana
233 Hammond Building
University Park, PA 16802

Kulite Semiconductor Products, Inc.
Attn: John R. Hayer
1039 Hoyt Avenue
Ridgefield, NJ 07657

Bolt Beranek and Newman, Inc.
Attn: Richard E. Hayden
50 Moulton Street
Cambridge, MA 02138

Air Force Wright Aeronautical
  Laboratory
Attn: Mr. Charles Bentz/POTC
Hot Section Technology
Wright Patterson AFB, OH 45433

AVCO Corporation
Attn: Mr. K. Collinge, Dir. of Research
IRAD Mechanical Projects Manager
Lycoming Division
550 South Main Street
Stratford, CT 06497

Eaton Corporation
Attn: Mr. Lamont Eltinge
P. O. Box 766
Southfield, MI 48037

Public Service Elect. & Gas Company
Attn: Dr. Melvin L. Zwillenberg
Research & Development Dept.
80 Park Plaza
Newark, NJ 07101

Raychem Corporation
Attn: Dr. David C. Chappelear
Director of Corporate Res. & Dev.
300 Constitution Drive
Menlo Park, CA 94025

Fabrication Development Laboratory
Attn: Mr. Hugh W. Bradley, Jr.
Owens/Corning Fiberglas
Technical Center
Granville, OH 43023

Xerox Electro-Optical Systems
Attn: Mr. Clifford I. Cummings
Manager, Intelligence & Reconnaissance
1616 North Fort Myer Drive, 16th Floor
Arlington, VA 22209

Construction Materials Support Group
Attn: Mr. J. W. Scott
Owens/Corning Fiberglas
CMG Process Technology Laboratory
Granville, OH 43023

Babcock & Wilcox R&D Division
Attn: Harold Wahle
P. O. Box 835
Alliance, OH 44601

Caterpillar Tractor Company
Attn: Mr. Donald Wilson
Technical Center, Building F
100 Northeast Adams Street
Peoria, IL 61629

NASA Headquarters
Attn: M/Paul N. Herr
Washington, DC 20546

Massachusetts Inst. of Technology
Attn: Dr. Alan Epstein, Rm. 31-266
Cambridge, MA 02139

Sverdrup (AEDC)
Attn: Paul McCarty
Arnold AFB, TN 37389

Rosemont, Inc.
Attn: Mr. Larry N. Wolfe
Mail Stop F-15
P. O. Box 959
Burnsville, MN 55337

Thermogage, Inc.
Attn: Charles E. Brookley
330 Allegany Street
Frostburg, MD 21534

Hycal Engineering
Attn: William Clayton
12105 Los Nietos Road
Sante Fe Springs, CA 90670

Medtherm Corporation
Attn: Larry Jones
P. O. Box 412
Hunstville, AL 35804

Rocketdyne
Attn: Dr. John C. Lee
6633 Canoga Avenue
Canoga Park, CA 91304

Combustion Engineering
Attn: John Fishburn
Dept. 9005-0301
Windsor, CT 06095

RdF Corporation
Attn: Frank Hines
23 Elm Avenue
Hudson, NH 03051

JEC Lasers, Inc.
Attn: Mr. John Wasko
253 Crooks Avenue
Patterson, NJ

NASA Langley Research Center
Attn: R. E. Wright, Jr. (MS-234)
Hampton, VA 23665

NASA Langley Research Center
Attn: S. L. Ocheltree (MS-235A)
Hampton, VA 23665

Babcock & Wilcox R&D Division
Attn: John Berthold
P. O. Box 835
Alliance, OH 44601

Applied Sensors International
Attn: Richard Stillmaker
7834 Palace Drive
Cincinnati, OH 45242

Carnegie-Mellon University
Attn: Dr. Norman Chigier
Dept. of Mechanical Engineering
Pittsburgh, PA 15213

Calspan Field Services, Inc./AEDC Div.
Attn: C. T. Kidd
Arnold Air Force Station, TN 37389

Physical Sciences Dept.
Attn: M. G. Dunn
Arvin/Calspan Adv. Tech. Ctr.
Buffalo, NY 14225

Eaton Corporation
Attn: Howard K. Cooper
Electronic Instrumentation Division
(Ailtech Strain Sensors)
5340 Alla Road
Los Angeles, CA 90066

Naval Air Propulsion Test Center
Attn: Guy Mangano/Code PE42
Trenton, NJ 08628

1. Report No. NASA CR-174833	2. Government Accession No.	3. Recipient's Catalog No.

4. Title and Subtitle	5. Report Date
High Temperature Static Strain Gage Alloy Development Program	March 1985
	6. Performing Organization Code

7. Author(s)	8. Performing Organization Report No.
C. O. Hulse, R. S. Bailey, F. D. Lemkey	R85-915952-13
	10. Work Unit No.
9. Performing Organization Name and Address	533-04-1A
United Technologies Corporation United Technologies Research Center East Hartford, CT 06108	11. Contract or Grant No.
	NAS3-23169
	13. Type of Report and Period Covered
12. Sponsoring Agency Name and Address National Aeronautics and Space Administration Lewis Research Center 21000 Brookpark Road Cleveland, Ohio 44135	Final Report
	14. Sponsoring Agency Code

16. Abstract

The literature, applicable theory and finally an experimental program were used to identify new candidate alloy systems for use as the electrical resistance elements in static strain gages up to 1250K. The program goals were 50 hours of use in the environment of a test stand gas turbine engine with measurement accuracies equal to or better than 10 percent of full scale for strains up to ± 2000 microstrain. As part of this effort, a computerized electrical resistance measurement system was constructed for use at temperatures between 300K and 1250K and heating and cooling rates of 250K/min and 10K/min. The two best alloys were an iron-chromium-aluminum alloy and a palladium base alloy. Although significicnat progress was made, it was concluded that a considerable additional effort would be needed to fully optimize and evaluate these candidate systems.

17. Key Words (Suggested by Author(s)) Strain Gages Elevated Temperature Alloys, Strain Gages Sensor Testing	18. Distribution Statement Star Category (35)

19. Security Classif. (of this report) Unclassified	20. Security Classif. (of this page) Unclassified	21. No. of Pages 47	22. Price*